Microcanonical unimolecular rate theory at surfaces. I. Dissociative chemisorption of methane on Pt(111)

A. Bukoski, D. Blumling, and I. Harrison[a]
Department of Chemistry, University of Virginia, Charlottesville, Virginia 22904-4319

A model of gas–surface reactivity is developed based on the ideas that (a) adsorbate chemistry is a local phenomenon, (b) the active system energy of an adsorbed molecule and a few immediately adjacent surface atoms suffices to fix microcanonical rate constants for surface kinetic processes such as desorption and dissociation, and (c) energy exchange between the local adsorbate–surface complexes and the surrounding substrate can be modeled via a Master equation to describe the system/heat reservoir coupling. The resulting microcanonical unimolecular rate theory (MURT) for analyzing and predicting both thermal equilibrium and nonequilibrium kinetics for surface reactions is applied to the dissociative chemisorption of methane on Pt(111). Energy exchange due to phonon-mediated energy transfer between the local adsorbate–surface complexes and the surface is explored and estimated to be insignificant for the reactive experimental conditions investigated here. Simulations of experimental molecular beam data indicate that the apparent threshold energy for CH_4 dissociative chemisorption on Pt(111) is $E_0 = 0.61$ eV (over a C–H stretch reaction coordinate), the local adsorbate–surface complex includes three surface oscillators, and the pooled energy from 16 active degrees of freedom is available to help surmount the dissociation barrier. For nonequilibrium molecular beam experiments, predictions are made for the initial methane dissociative sticking coefficient as a function of isotope, normal translational energy, molecular beam nozzle temperature, and surface temperature. MURT analysis of the thermal programmed desorption of CH_4 physisorbed on Pt(111) finds the physisorption well depth is 0.16 eV. Thermal equilibrium dissociative sticking coefficients for methane on Pt(111) are predicted for the temperature range from 250–2000 K. Tolman relations for the activation energy under thermal equilibrium conditions and for a variety of "effective activation energies" under nonequilibrium conditions are derived. Expressions for the efficacy of sticking with respect to normal translational energy and vibrational energy are found. Fractional energy uptakes, f_j, defined as the fraction of the mean energy of the complexes undergoing reaction that derives from the jth degrees of freedom of the reactants (e.g., molecular translation, vibration, etc.) are calculated for thermal equilibrium and nonequilibrium dissociative chemisorption. The fractional energy uptakes are found to vary with the relative availability of energy of different types under the specific experimental conditions. For thermal dissociative chemisorption at 500 K the fractional energy uptakes are predicted to be $f_t = 13\%$, $f_r = 18\%$, $f_v = 33\%$, and $f_s = 36\%$. For this equilibrium scenario relevant to catalysis, the incident gas molecules supply the preponderance of energy used to surmount the barrier to chemisorption, $f_g = f_t + f_v + f_r = 64\%$, but the surface contribution at $f_s = 36\%$ remains significant. © *2003 American Institute of Physics.* [DOI: 10.1063/1.1525803]

I. INTRODUCTION

Understanding the mechanisms and kinetics of surface chemistry is central to advancing technology derived from many fields, ranging from catalysis and corrosion inhibition, to device physics, materials science, nanotechnology, and tribology. Although the investigation of nonequilibrium and kinetically controlled surface phenomena induced by molecular, electron, and photon beams is an active research frontier,[1] there has been relatively little exploration of simple statistical theories[2–4] to model these systems. In this paper, we describe a general framework for analyzing and predicting both thermal equilibrium and nonequilibrium kinetics for surface reactions. Specifically, an earlier microcanonical

unimolecular rate theory for activated dissociative chemisorption[5] is implemented in a more computationally exact manner and is expanded within a Master equation approach to explicitly account for vibrational energy transfer with the surface. The central tenets of the model are that (a) adsorbate chemistry is a local phenomenon, (b) the active system energy of an adsorbed molecule and a few immediately adjacent surface atoms suffices to fix microcanonical rate constants for surface kinetic processes such as desorption and dissociation, and (c) energy exchange between the local adsorbate-surface complexes and the surrounding substrate can be modeled via a Master equation to describe the system/heat reservoir coupling (see Fig. 1).

Activated dissociative chemisorption of molecules on metal surfaces is the rate-limiting step for many catalytic

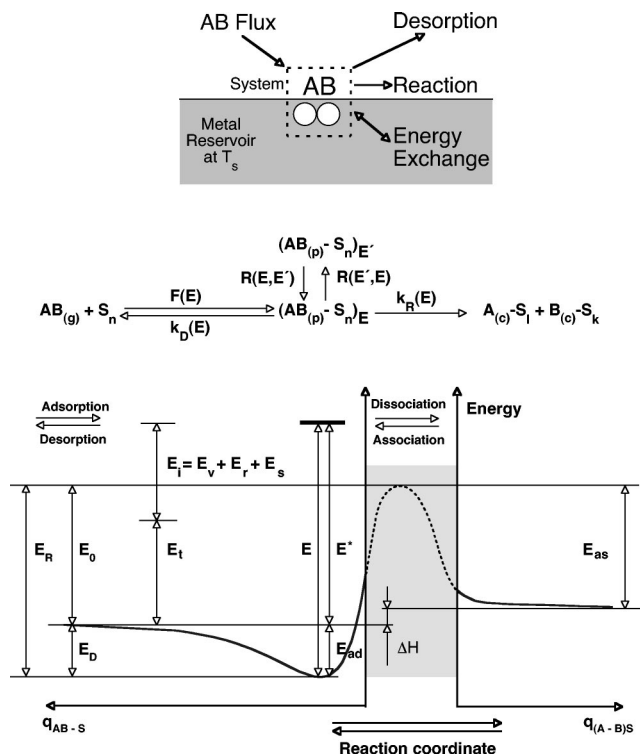[a]Electronic mail: harrison@virginia.edu

     843

FIG. 1. Schematic depiction of the kinetics and energetics of activated dissociative chemisorption. Zero-point energies are implicitly included within the potential energy curve along the reaction coordinate. Refer to the text for further details.

syntheses of industrial importance and these reactions are sufficiently simple to be attractive model systems for study by the chemical physics community. Although activated dissociative chemisorption, such as H_2 on $Cu(111)$[6] and CH_4 on a variety of metal surfaces,[7,8] has been investigated for some years, there remains little apparent consensus as to when a dynamical theory or a statistical theory is most appropriate to make connection with experiment.[9] Impressive progress in the electronic structure theory (EST) of metal surfaces makes it possible to calculate reasonable transition state structures, energies, and normal mode frequencies for catalytic reactions[10,11]—but it has been difficult to experimentally test the accuracy of these calculations. Although the multidimensional and sometimes quantum-state resolved dissociative sticking data derived from molecular beam or associative desorption experiments can usually be summarized using empirical fitting forms, no rigorous connection has been made between the resulting experimental fit parameters and the reaction barrier height and other quantities that can be directly calculated by EST.[12] Extrapolating from what is known about gas-phase reaction dynamics,[13] one anticipates that statistical Rice–Ramsperger–Kassel–Marcus (RRKM) theory should suffice to describe the dissociative chemisorption of most polyatomic molecules although dynamical effects may be important for smaller molecules where intramolecular vibrational energy redistribution (IVR) can be negligible. Nevertheless, dynamical effects in surface kinetics may be unusual to observe even for the smallest molecules because the low frequency phonon and local adsorbate-surface modes introduced when a molecule interacts with a surface will enhance IVR rates relative to those of an isolated molecule in the gas phase. Finally, it is worth noting that in the gas phase, microcanonical rate theory can quantitatively predict detailed rates for most adiabatic reactions,[14] including even the hydrogen exchange reaction, $H_{(g)} + H_{2(g)} \rightarrow H_{2(g)} + H_{(g)}$,[15] a reaction that proceeds without any deep potential wells in the neighborhood of the transition state that might support long lived intermediates.[16] In this paper, we implement a microcanonical transition state theory of dissociative chemisorption whose free parameters can be fixed through iterative simulation of varied experimental data or calculated directly by EST, thereby establishing a clear and quantitative connection between the results of experiment and EST.

Evaluation of the quantitative applicability of any surface kinetics theory is challenging because experimental dissociative sticking coefficients measured in different laboratories can differ by as much as an order of magnitude,[17] and the accuracy of transition state energetics derived from EST remains the subject of lively debate.[18,19] In consequence, we choose to develop a surface kinetics theory with a minimum number of adjustable parameters with the foreknowledge that RRKM rate expressions[13] are notoriously insensitive to the choice of all but the lowest vibrational mode frequencies in the transition state and very sensitive to the choice of reaction barrier height. As will be seen, a three-parameter model for dissociative chemisorption of methane on $Pt(111)$ can adequately predict the results of all 62 initial sticking measurements made at IBM over a wide range of molecular beam conditions. For $CH_4/Pt(111)$ the three-parameters are the apparent threshold energy for dissociation, $E_0 = 0.61$ eV (over a C–H stretch reaction coordinate); a lumped low frequency representative of the $CH_4 - Pt$ stretching mode along the surface normal and the frustrated rotations within the physisorption potential well, $\nu_D = 110$ cm^{-1}; and the number of surface vibrational modes that can freely exchange energy in the local adsorbate–surface complex, $s = 3$. The theoretical analysis supports the notion that the $CH_4/Pt(111)$ reactive potential energy surface has 16 active degrees of freedom and it is encouraging that a considerably smaller number of parameters (3) suffices to predict the varied surface kinetics in quantitative fashion.

Throughout this paper, we assume that activated dissociative chemisorption on metals occurs adiabatically on a single Born–Oppenheimer potential energy surface. Energy transfer between the adsorbate–surface complexes and the underlying substrate is assumed to occur through phonon mediated vibrational energy exchange. There is no explicit accounting for the possibility that electron–hole ($e-h$) pair creation may accompany molecular adsorption.[20] Nor is there any explicit provision for coupling $e-h$ pair creation in the metal to adsorbate vibrational modes as is known to be significant for the vibrational relaxation of the high frequency stretching mode of CO on $Cu(111)$.[1]

To thoroughly understand molecular beam studies of activated dissociative chemisorption it will be useful to briefly review thermalized trapping-mediated dissociative chemisorption prior to treating direct dissociative chemisorption. Our Master equation approach towards activated dissociative

chemisorption will be seen to encompass trapping-mediated dissociative chemisorption as a limiting case.

II. THERMALIZED TRAPPING-MEDIATED DISSOCIATIVE CHEMISORPTION

Following Weinberg,[21] let us first consider the kinetics of thermalized trapping-mediated dissociative chemisorption of a molecule AB on a metal surface,

$$AB_{(g)} \underset{k_D}{\overset{\zeta F}{\rightleftharpoons}} AB_{(p)} \overset{k_R}{\rightarrow} A_{(c)} + B_{(c)}, \tag{1}$$
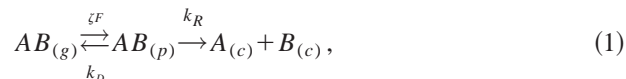
where AB can exist as a weakly bound physisorbed molecule or as dissociated chemisorbed fragments on the surface. The initial trapping probability, ζ, is the probability for an initial flux of molecules, F, incident on a clean surface to become trapped in the physisorption well for sufficient time that the molecules become accommodated to the surface temperature. After trapping, the thermalized $AB_{(p)}$ can go on to react (dissociatively chemisorb) or desorb with thermal rate constants k_R and k_D. If the $(1-\zeta)$ fraction of the incident flux which does not trap essentially bounces off the surface with relatively little probability for dissociation, then an initial sticking coefficient can be derived on the basis of the Eq. (1) kinetics above. Applying the steady state approximation to the coverage of trapped and thermalized physisorbed molecules, θ_p,

$$\frac{d\theta_p}{dt} = \zeta F - (k_R + k_D)\theta_p \cong 0, \tag{2}$$

defines the reactive flux as

$$\frac{d\theta_c}{dt} = k_R \theta_p^{ss} = \frac{\zeta k_R}{k_R + k_D} F = S F, \tag{3}$$

and the sticking coefficient as

$$S = \frac{\zeta k_R}{k_R + k_D} = \zeta \left(1 + \frac{k_D}{k_R}\right)^{-1}$$
$$= \zeta \left(1 + \frac{A_D}{A_R} \exp\left[-\frac{E_{aD} - E_{aR}}{k_b T_s}\right]\right)^{-1}, \tag{4}$$

where ζ is a dynamical parameter dependent on the details of the incident flux and k_R and k_D are thermal rate coefficients of the Arrhenius form, $k_i(T_s) = A_i \exp(-E_{ai}/k_b T_s)$, that depend on the surface temperature. Molecular beam experiments are typically required to experimentally determine the behavior of $\zeta = \zeta(E_t, T_s)$ which depends on the translational (and possibly the internal) energy of the incident molecules and the surface temperature. The overall kinetics contains, at a minimum, three independent parameters to be determined. The trapping model has been applied to numerous C_2 and higher alkanes on a variety of Ir, Ru, and Pt substrates[22] under conditions where the initial trapping probability is large (i.e., thermal incident energies or translational energies $E_t \lesssim 0.5$ eV) and the activation energy for reaction, E_{aR}, is apparently smaller than that for desorption, E_{aD}. Very recently there have been reports that methane at low transla-

tional energies can also undergo trapping-mediated dissociative adsorption on certain Ir and Pt surfaces even though $E_{aR} > E_{aD}$ for this molecule.[23]

At sufficiently high E_t and T_s, the trapping probability for thermalization of the incident molecules tends to zero and "direct" dissociation kinetics may dominate in which there is no apparent thermalization of the incident molecules. Under these conditions, there is insufficient energy exchange with the surface and the lifetime of the molecule on the surface is too short for efficient thermalization to the surface temperature. The $(1-\zeta)$ fraction of the incident flux that is not completely trapped and thermalized can undergo up to a few relatively high energy collisions/oscillations with the surface prior to desorption and these provide the opportunity for "direct" dissociation. For dissociative adsorption systems for which $E_{aR} \gg E_{aD}$, the direct dissociation channel is likely to dominate any thermalized precursor mediated dissociation because a thermalized adsorbate is much more likely to desorb then to react [i.e., $S \rightarrow 0$ in Eq. (4)]. Kinetic analysis of direct dissociation involving energetic and incompletely thermalized reagents cannot employ familiar Arrhenius thermal rate constants but rather requires a more detailed microcanonical or full dynamical treatment of the reactive system.

III. MASTER EQUATION FOR ACTIVATED DISSOCIATIVE CHEMISORPTION

Let us now restrict our attention to activated dissociative chemisorption systems of the kind depicted schematically in Fig. 1 for which $E_R \gg E_D$ [e.g., CH_4 on Pt(111)] and the dissociation kinetics are direct. We will assume that the chemistry is local and involves the collisional formation of an energized complex consisting of a physisorbed molecule and a few surface atoms that can go on to react, desorb, or exchange energy with the substrate. *State densities at reactive energies should be sufficiently high [e.g., 10^6 per cm^{-1} at E_R for $CH_4/Pt(111)$] that dissociation rates will depend on the total energy, E, of the energized complex rather than on any dynamical propensity to react from favored quantum states.* The high state density at energies relevant to reactive processes ($E \geq E_R$) also means that any collision that could lead to reaction is likely to efficiently and randomly mix the energy of the incident molecule and that of the few surface atoms of the physisorbed complex. Because our primary interest is in calculating dissociative sticking coefficients, we will simply assume that when a molecule initially collides with the surface full statistical energy mixing occurs (subject to applicable conservation laws). If this postulate breaks down at energies less than E_R it will influence low energy desorption rates but it should have relatively little effect on the calculated dissociative sticking coefficients. Finally, we allow for vibrational energy exchange between the energized complexes and the surrounding metal such that detailed balance applies and the complexes can be equilibrated to the surface temperature under appropriate conditions. These assumptions lead to a microcanonical rate theory based on the following Master equation for the time evolution of the coverage of physisorbed complexes at energy E in increment of energy dE, $\theta_p(E,t)dE$,

$$\frac{d\theta_p(E,t)}{dt}dE = F(E,t)dE - \{k_R(E) + k_D(E)\}\theta_p(E,t)dE$$

$$+ \int_0^{\infty} \{R(E,E')\theta_p(E',t)dE$$

$$- R(E',E)\theta_p(E,t)dE\}dE', \qquad (5)$$

where $F(E,t)dE$ represents an external flux that forms physisorbed complexes at energy E, $k_R(E)$, and $k_D(E)$ are microcanonical rate constants for reaction and desorption, and pseudo-first-order rate constants of the form $R(E,E')$ govern the vibrational energy exchange with the metal that transfers energized complexes at energy E' to energy E. It is worth noting that, although in this paper the $F(E,t)$ source term for forming energized complexes at energy E will derive from the collisional flux from an impinging molecular beam or ambient gas, $F(E,t)$ could equally well represent a source term for energized complexes derived from electron or photon induced excitation of molecules already physisorbed at low temperature.

A. Energy distribution of physisorbed complexes

Theory[24–28] and experiment[29] on multiphonon scattering of rare gases from smooth close packed metal surfaces find that the gas momentum parallel to the surface is largely conserved. Parallel momentum conservation derives from a lack of corrugation of the interaction potential parallel to the surface and typically breaks down for geometrically rougher, more open surfaces that possess more corrugated interaction potentials. Dissociative chemisorption studies of methane[30] and hydrogen[6] incident on some close packed metal surfaces have found that dissociative sticking scales with the molecular translational energy directed normal to the surface, $E_n = E_t \cos^2(\vartheta)$, where ϑ is the angle of incidence away from the surface normal. This "normal energy" reactive scaling suggests that parallel momentum is conserved over the time scale of a reactive collision on a smooth surface and that only the normal translational energy is effective in promoting reaction.

Trajectory calculations[31] for Ar scattering from Pt(111) at high temperatures found that Ar often undergoes quasi-equilibrium trapping/desorption for which desorption occurs after thermalization of the normal momentum but before the parallel momentum can be equilibrated to the surface temperature. The calculated time for thermalization of parallel momentum for the Ar/Pt(111) system is quite long, 84 ps at 273 K, which is roughly twice the time required for desorption. Under such conditions of quasiequilibrium desorption, with incomplete thermalization of parallel momentum, standard assumptions for experimental analysis of trapping probabilities, $\zeta(E_t, T_s)$, may fail.[1,31] Memory retention of the incident parallel momentum skews the trapping/desorption angular distribution away from $\cos(\vartheta)$ and into the angular lobe of the direct inelastic scattering channel making clean experimental separation of the trapping channel difficult, if not impossible. This can lead to apparent ζ scaling with $E_t \cos^n(\vartheta)$ with artificially variable n with T_s, even though strict normal energy scaling ($n=2$) of the trapping (i.e., thermalization of the normal momentum) always applies at the

microscopic level.[32] Extrapolating to reactive systems, there may be some systems whose reactivity obeys normal energy scaling but whose apparent trapping behavior does not. We will assume in such cases that parallel momentum is conserved over the duration of the reactive collision, a time period fixed by the desorption rate at energies $E \gtrsim E_R$.

Conservation of molecular angular momentum directed along the surface normal may introduce another constraint on collisional energy exchange for smooth surfaces if relatively uncorrugated interaction potentials produce insignificant in-plane torques. We ignore such possibilities here.

Unless subject to additional conservation laws, we assume that when a gas molecule collides with the surface full statistical energy mixing occurs within the physisorbed complex formed of the molecule and a local cluster of a few surface atoms. Following the energetics of Fig. 1, the freely exchangeable energy E of the physisorbed complex is

$$E = E_s + E_t + E_v + E_r + E_{\text{ad}}, \qquad (6)$$

where E_s is the vibrational energy of the cluster of surface atoms, E_t, E_v, and E_r are the translational, vibrational, and rotational energies of the incident molecule, respectively, and E_{ad} is the adsorption energy. The adsorption energy is equal to the desorption energy, E_D, if there is no barrier to desorption that rises above the asymptotic energy for a molecule at rest at infinite separation from the surface (as in Fig. 1). If parallel momentum is conserved only the normal component of the translational energy, $E_n = E_t \cos^2(\vartheta)$, contributes to E as "E_t" in Eq. (6).

Molecules striking a surface from a supersonic molecular beam have a nonequilibrium energy distribution which is typically characterized by the beam's mean translational energy, $\langle E_t \rangle$, and its translational, T_t, vibrational, T_v, and rotational, T_r, temperatures. The vibrational energy distribution of the metal surface atoms before impact of a molecule is governed by the surface temperature, T_s. Consequently, besides the beam's mean translational energy, four independent temperatures play a role in fixing the energy available in a gas-surface collision: T_t, T_v, T_r, and T_s. The flux of physisorbed complexes formed with energy E is given by

$$F(E) = \int_0^{E - E_{\text{ad}}} f_i(E_i) F_t(E - E_i) dE_i$$

$$= F_0 \int_0^{E - E_{\text{ad}}} f_i(E_i) f_t(E - E_i) dE_i = F_0 f(E), \qquad (7)$$

where

$$f_i(E_i) = \int_0^{E_i} f_s(E_s) \int_0^{E_i - E_s} f_v(E_v) f_r(E_i - E_s - E_v) dE_v \, dE_s, \qquad (8)$$

is the probability distribution for forming a physisorbed complex with internal energy, E_i,

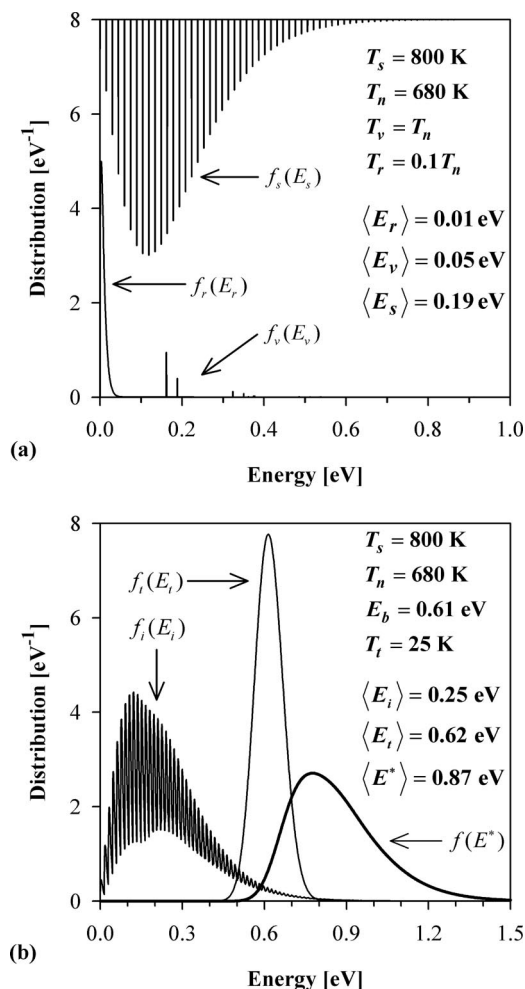$$E_i = E_s + E_v + E_r, \qquad (9)$$

(a)

(b)

FIG. 2. (a) Rotational, vibrational, and surface energy distributions associated with a molecular beam of CH_4 incident on Pt(111) along the direction of the surface normal under conditions typical for dissociative sticking experiments. These distributions are scaled such that the maximum value is 5 units high and the surface energy distribution is inverted for clarity. (b) Normalized translational energy distribution of the incident CH_4 beam and the normalized internal and total energy (E^*) distributions of the physisorbed complexes under the typical experimental conditions of (a).

given canonical probability distributions $f_s(E_s)$, $f_v(E_v)$, and $f_r(E_r)$ for the surface vibrational energy and the molecule's vibrational energy and rotational energy, respectively. The molecular flux distribution incident on the surface is $F_t(E_t) = F_0 f_t(E_t)$ where F_0 is the net molecular flux incident on the surface in monolayers/s and $f_t(E_t)$ is the molecules' flux weighted translational energy distribution. The normalized flux distribution for creation of physisorbed complexes with energy E is $f(E)$. If parallel momentum is conserved over the reactive collision then only normal translational energy is included in E and $f_t(E_t)$ is replaced by the flux distribution for normal translational energy.

Figure 2 provides a representative example of the physisorbed complex $f(E^*)$, where $E^* = E - E_{ad}$, and the assembly of $f(E^*)$ by convolution from the canonical distributions $f_s(E_s)$, $f_v(E_v)$, $f_r(E_r)$, and $f_t(E_t)$ appropriate for a molecular beam of CH_4 impinging on a Pt(111) surface under typical experimental conditions for measurements of dissociative sticking. Even though the translational temperature of the

CH_4 molecular beam is only $T_t = 25$ K in this example, the breadth of the collision induced physisorbed complex flux distribution, $f(E^*)$, is quite broad (fwhm = 0.34 eV). In dissociative sticking experiments, $f(E)$ is typically scanned over a range of E where dissociative chemisorption is possible by (a) varying the mean translational energy, $\langle E_t \rangle$, and T_t of the molecular beam by seeding in various carrier gases and/or by changing the beam nozzle temperature, T_n, (b) varying T_n to exert control over T_v and T_r, or (c) varying the surface temperature, T_s.

B. Microcanonical rate constants

The microcanonical rate constants for reaction and desorption, k_R and k_D, are of the usual RRKM form[33,34]

$$k_i(E) = \frac{W_i^\ddagger(E - E_i)}{h\ \rho(E)}, \tag{10}$$

where $W_i^\ddagger$ is the sum of states for transition state i, h is Planck's constant, and ρ is the physisorbed complex density of states. Symmetry factors for rotational motions, σ, should be built into the ρ's and W's for the transitions states and physisorbed complex in order to consistently implement the Eq. (5) Master equation.[33] Symmetry factors account for classical over-counting of rotational states in high symmetry molecules with indistinguishable atoms such that $\rho = \rho_{distinguishable}/\sigma$ (where, for example, $\sigma = 2$ for $H_{2(g)}$ and $\sigma = 12$ for $CH_{4(g)}$). Reaction path statistical factors[35] should not be incorporated into the microcanonical rate constants as a substitute for consistent implementation of the symmetry factors.

Transition states for dissociative chemisorption of polyatomic molecules typically involve multiple coordination to the surface because the optimal energetics usually occur as the dissociating intramolecular bond is only fractionally broken and the separating fragments are beginning to form partial new bonds to the surface atoms. This usually leads to rotationally and translationally constrained transition states with no overall symmetry. Such reactive transition states can be described as a collection of oscillators with a symmetry factor of 1.

C. Vibrational energy exchange with the surrounding solid

Vibrational energy transfer between the physisorbed complexes and the surrounding metal is governed by rate coefficients $R(E,E')$ which can be expressed as a product of the total inelastic collision frequency, ω, multiplied by the collision step-size distribution, $P(E,E')$,[36]

$$R(E,E')dE = \int_0^\infty R(E,E')dE \left\{ \frac{R(E,E')}{\int_0^\infty R(E,E')dE} \right\} dE$$

$$= \omega P(E,E')dE, \tag{11}$$

where ω is the integral over the rates of all inelastic transitions from initial energy E' to final energy E, and the quantity in braces is $P(E,E')$, sometimes also called the prob-

ability of energy transferred per collision. The separation of $R(E,E')$ into the $\omega P(E,E')$ product is done for convenience because neither ω nor $P(E,E')$ occur separately from one another and only $R(E,E')$ need appear in the Master equation. Nevertheless, the factorization of $R(E,E')$ provides a useful physical picture for the energy transfer and establishes connection to vibrational energy transfer studies in the gas phase. In the spirit of Fig. 1, for the physisorbed complexes at the surface ω is anticipated to be close to three times the mean phonon frequency [e.g., $\omega = 3 \times (3.7 \times 10^{12} \text{ s}^{-1})$ for Pt][31] of the metal given that phonons bathe the complexes from three independent directions. If there proves to be a bottleneck to rapid energy exchange with the metal, the molecule/surface stretching vibration in the direction of the surface normal might be a reasonable alternative candidate to consider for ω. With a consistent choice of ω, the Eq. (11) definition implies that the collision step-size distribution is normalized,

$$\int_0^\infty P(E,E') dE = 1. \tag{12}$$

The requirement of detailed balance of the upward and downward rates of collisional energy transfer for an equilibrium population of physisorbed complexes at the surface temperature, $\theta_p(E,t;T_s)$, constrains the form of the $R(E,E')$,

$$R(E,E') \theta_p(E',t;T_s) = R(E',E) \theta_p(E,t;T_s), \tag{13}$$

and ensures that the Eq. (5) Master equation provides for no net collisional energy transfer for a distribution of physisorbed complexes in thermal equilibrium with the surface. At thermal equilibrium, the physisorbed complexes are distributed according to the Boltzmann distribution,

$$\theta_p(E,t;T_s) = \theta_p(t) \frac{\rho(E)\exp(-E/k_b T_s)}{Q(T_s)} = \theta_p(t) \frac{B(E)}{Q(T_s)}, \tag{14}$$

where $\theta_p(t)$ is the total coverage of physisorbed complexes and $\rho(E)$, $Q(T_s)$, and $B(E)$ are the physisorbed complex density of states, partition function, and Boltzmann weighting factor, respectively, for active degrees of freedom contributing to the freely exchangeable energy E. Substituting for $\theta_p(E,t;T_s)$ in Eq. (13) yields the detailed balance constraint,

$$\frac{R(E,E')}{R(E',E)} = \frac{P(E,E')}{P(E',E)} = \frac{\rho(E)}{\rho(E')} \exp\left\{-\frac{E-E'}{k_b T_s}\right\} = \frac{B(E)}{B(E')}. \tag{15}$$

Although there is a long history of investigation of vibrational energy transfer in bimolecular gas phase collisions,[33,34,36] relatively little information is known about the detailed form that $P(E,E')$ should take. Some of the models for $P(E,E')$ motivated by theoretical considerations are the stepladder,[37] Gaussian,[37] and biased random walk[38] models. In this paper, we will employ a variant of the most widely used "exponential down" model[39] for which the exponential dependence of the vibrational energy transfer probability on the energy gap between levels can be broadly rationalized on the basis of both classical and quantum mechanical analysis of intermolecular collisions.[40] Here, we use a "density weighted-exponential down" energy transfer model that is relatively easy to implement and simple in concept. For downwards transitions from E' to E,

$$P(E,E') = \frac{\rho(E)}{N(E')} \exp\left\{-\frac{E'-E}{\alpha}\right\} \quad \text{for } E' > E, \tag{16}$$

where $N(E')$ is a normalization constant and α is a parameter that may depend on the initial energy E'. Consequently, the probability for undergoing a downwards energy transfer from E' to E is exponentially damped in the energy gap, $\Delta E = E' - E$, and proportional to the number of final states, $\rho(E)dE$ in dE at E, that are available to land in. The collision step-size distribution for upwards transitions is determined by the Eq. (15) detailed balance requirement,

$$P(E,E') = \frac{\rho(E)}{N(E)} \exp\left\{-\left(\frac{1}{\alpha} + \frac{1}{k_b T_s}\right)(E-E')\right\}$$
$$\text{for } E > E'. \tag{17}$$

Determination of the energy dependent $N(E')$ is worth discussing more generally. For several energy transfer models the downward collision step-size distribution has the form

$$P(E,E') = \frac{1}{N(E')} r(E,E') \quad \text{for } E' > E, \tag{18}$$

where $N(E')$ is a normalization constant and $r(E,E')$ is some particular function (e.g., exponential, Gaussian, etc.). The $P(E,E')$ for upwards transitions is fixed uniquely by detailed balance after the initial specification of the downward $P(E,E')$. In consequence, the Eq. (12) normalization of the global $P(E,E')$ can be used to derive an integral equation for $N(E')$,[34]

$$N(E') = \frac{\int_0^{E'} r(E,E') dE}{1 - \frac{1}{B(E')} \int_{E'}^{\infty} \frac{B(E)}{N(E)} r(E',E) dE}, \tag{19}$$

that depends explicitly on only the downward collision step-size distribution.

In the density weighted-exponential down model of vibrational energy transfer, α is closely related to the average energy transferred in downwards collisions $\langle \Delta E(E') \rangle_d$, which is a commonly reported measure for summarizing energy transfer efficiency in the gas-phase,

$$\langle \Delta E(E') \rangle_d = \frac{\int_0^{E'} (E'-E) P(E,E') dE}{\int_0^{E'} P(E,E') dE}. \tag{20}$$

If α is a function of the initial state energy E' alone, $\alpha(E')$ is roughly equal to $\langle \Delta E(E') \rangle_d$, for $E' \gg 0$. Barker's recommendation[36] for estimating α for gas-phase molecules similar in size to benzene, in the absence of specific experimental vibrational energy transfer information, is to set,

$$\alpha(E') = c_0 + c_1 E', \tag{21}$$

where $c_0 \sim 40$ cm^{-1} and c_1 varies with the identity of the molecular collision pairs. For example, Eq. (21) is followed quite well for pyrazine and when this molecule collides with itself or with CO_2, $\alpha(10\ 000$ cm$^{-1})$ is 393 and 168 cm^{-1}, respectively.[41] To restrain the surface kinetics theory to a minimum number of adjustable parameters, we will initially assume that vibrational energy transfer between the physisorbed complexes and the surrounding metal is mediated by phonons impinging/outgoing from three independent directions and take ω equal to 3 times the mean phonon frequency, 1.1×10^{13} s^{-1}, and α equal to the mean phonon energy, 122 cm^{-1}, of Pt [n.b. $\alpha \neq \alpha(E')$]. In the Debye model of solids the mean phonon energy is $\frac{3}{4} k_b T_{\text{Debye}}$, where T_{Debye} is the Debye temperature.

Some recent experimental studies of gas phase vibrational energy transfer detect the presence of a small number of "supercollisions" that involve energy transfers on the order of $10\ k_b T$ or higher which can lead to a biexponential $P(E, E')$ with a significant high ΔE tail.[42] Although the presence of a small quantity of supercollisions might lead to increased reactivity at low temperatures and low incident translational energies in activated dissociative chemisorption on surfaces, in this paper we ignore supercollisions and employ the simpler density weighted single exponential down energy transfer model.

Replacing the vibrational energy transfer rate coefficients, $R(E, E')$, in favor of the collision step-size distributions, $P(E, E')$, the Eq. (5) Master equation can be rewritten as

$$\frac{d\theta_p(E, t)}{dt} = F(E, t) - \{k_R(E) + k_D(E) + \omega\}\theta_p(E, t)$$

$$+ \omega \int_0^\infty P(E, E')\theta_p(E', t)\ dE'. \qquad (22)$$

D. Dissociative sticking coefficient

Our earlier microcanonical unimolecular rate theory[5] for dissociative chemisorption neglected vibrational energy transfer between the physisorbed complexes and the surface. This simpler theory is recovered if all vibrational energy transfer terms are truncated from the Master equations (5) or (22) to give

$$\frac{d\theta_p(E, t)}{dt} = F(E, t) - \{k_R(E) + k_D(E)\}\theta_p(E, t). \qquad (23)$$

Within the framework of the reaction scheme of Fig. 1, let us find an expression for the initial sticking coefficient, S, when a time-independent flux F_0 is made incident on a clean surface and $d\theta_c/dt = S F_0$ describes the initial increase in coverage of either of the chemisorbed dissociation fragments. Applying the steady state approximation to the physisorbed complex coverage distribution at E [i.e., setting Eq. (23) $= 0$] allows us to define the reactive flux at E as

$$\frac{d\theta_c(E)}{dt} = k_R(E)\theta_p^{ss}(E) = \frac{k_R(E)}{k_R(E) + k_D(E)}F(E) \qquad (24)$$

$$= S(E)F(E),$$

where $\theta_c(E)$ is the coverage distribution of either of the chemisorbed dissociation fragments at E and $S(E)$ is the microcanonical sticking coefficient. Rearranging and writing the collision flux distribution as $F(E) = F_0 f(E)$ [as in Eq. (7)] leads to the operational definition of the experimentally realized sticking coefficient,

$$S = \frac{1}{F_0}\frac{d\theta_c}{dt} = \frac{1}{F_0}\int_0^\infty \frac{d\theta_c(E)}{dt}dE = \int_0^\infty S(E)f(E)dE, \qquad (25)$$

which is simply the microcanonical sticking coefficient averaged over the probability of forming a physisorbed complex at E.

This simplest physisorbed complex (PC) microcanonical unimolecular rate theory (MURT) provides a consistent analysis and prediction framework for both equilibrium and nonequilibrium dissociative chemisorption experiments (even at fully quantum state resolved levels).[5] To date, the PC–MURT has enjoyed apparent quantitative success in handling the dissociative chemisorption from molecular beams of: methane on Pt(111),[5] silane on Si(100),[43] and germane on Ge(100) and Ge(111).[44] Application to the dissociation of larger alkanes on Pt(111) was not as successful and only the qualitative reactivity trends with increasing alkane complexity were predicted.[45] Another apparent quantitative failure for the PC–MURT concerned its detailed balance predictions for the translational energy distribution and angular distribution for the methane reaction product from the laser-induced thermal hydrogenation of methyl radicals on Pt(111) (i.e., the reverse reaction of methane dissociative chemisorption under thermal equilibrium conditions).[46] However, quantitative agreement between theory and experiment was recovered when the threshold energy for CH_4/Pt(111) dissociative chemisorption was allowed to vary from $E_0 = 0.63$ to 1.2 eV as the coverage of $H + CH_3$ on the surface was varied from 0 in the molecular beam experiments to close to full coverage in the laser induced thermal reaction experiments.[47] Arguing along Evans–Polanyi lines,[48] that as the reaction products are destabilized so too is the transition state, the threshold energy to methane dissociation should increase when a clean surface is tempered by an increasing coverage of chemisorbed species. Nevertheless, a doubling of the threshold energy as the chemisorbed $H + CH_3$ coverage increases towards saturation may represent an unrealistically rapid rate of increase.

When the PC–MURT is evaluated in a more computationally exact manner (e.g., by employing full state counting, eliminating an approximation to describe the rotational states of the desorption transition state, consistently implementing symmetry factors, etc.) as compared to earlier studies, the methane molecular beam sticking predictions are quantitatively nearly identical but the detailed balance predictions show some significant changes as will be documented in a later paper.

Despite some success in interpreting experiments, it is worth pointing out explicitly that the PC–MURT is theoretically crippled by its neglect of vibrational energy transfer with the surface and this leads to complete independence from the adsorption energy of the physisorbed molecules

(i.e., there is no mechanism to trap into the physisorption well). To clarify the last assertion, first notice that the microcanonical sticking coefficient,

$$S(E) = \frac{k_R(E)}{k_R(E) + k_D(E)} = \frac{W_R^{\ddagger}(E - E_R)}{W_R^{\ddagger}(E - E_R) + W_D^{\ddagger}(E - E_D)}, \quad (26)$$

based on the Eq. (10) rate coefficients depends only on the sums of states for the reaction and desorption transition states (after cancellation of the density of states for the physisorbed complexes). Choosing an alternate energy floor for the physisorbed complexes where the molecule is at infinite separation from the surface, the energy of a complex can be written as $E^* = E - E_{ad}$. It is then possible to rewrite Eq. (26) as

$$S(E^*) = \frac{W_R^{\ddagger}(E^* - E_0)}{W_R^{\ddagger}(E^* - E_0) + W_D^{\ddagger}(E^*)}, \quad (27)$$

and Eq. (7) as

$$F(E^*) = F_0 \int_0^{E^*} f_i(E_i) f_t(E^* - E_i) \, dE_i = F_0 \, f(E^*), \quad (28)$$

such that the experimental sticking coefficient

$$S = \int_0^{\infty} S(E^*) \, f(E^*) \, dE^*, \quad (29)$$

can be calculated without any reference to the adsorption energy whatsoever.

E. Solving the Master equation

A formal solution for the experimentally realized sticking coefficient from a molecular beam experiment beginning with the Eq. (22) Master equation in the steady state approximation is

$$S = \frac{1}{F_0} \frac{d\theta_c}{dt} = \int_0^{\infty} \frac{k_R(E)}{k_R(E) + k_D(E) + \omega}$$
$$\times \left(f(E) + \frac{\omega}{F_0} \int_0^{\infty} P(E, E') \, \theta_p^{ss}(E') \, dE' \right) dE, \quad (30)$$

$$S = \int_0^{\infty} S_{\omega}(E) \, f_c(E) \, dE, \quad (31)$$

where the microcanonical sticking coefficient, $S_{\omega}(E)$, now correctly represents that there are three ways for a physisorbed complex formed at energy E to decay: to react, to desorb, or to exchange energy with the surface. The unnormalized cumulative flux distribution to form a physisorbed complex at E is given by $f_c(E)$, the trailing term in braces in Eq. (30). Interestingly, since the collisional flux distribution $f(E)$ is already normalized to 1, $f_c(E)$ integrated over E can be greater than 1. This is possible because there are multiple opportunities to form a physisorbed complex at energy E; either directly from an initial gas–surface collision or afterwards through vibrational energy transfer with the surface. Ultimately, as for the simple PC–MURT, the experimentally

realized sticking coefficient can be derived from a microcanonical sticking coefficient averaged over the cumulative probability for forming a physisorbed complex at E.

Analytic solution of the Eq. (22) Master equation for the time dependent population of physisorbed complexes is not generally feasible. Nevertheless, the Master equation can be reformulated in matrix form and solved numerically for realistic systems. The first step towards a numeric solution is to partition the energy levels into a contiguous set of energy grains. Each grain may be thought of as an energy-grained state, associated with an effective degeneracy and an appropriately weighted energy and rate constant. Following the graining procedure outlined by Holbrook et al.,[33] we arrive at the energy grained Master equation (EGME),

$$\frac{d\theta_i(t)}{dt} = F_i(t) - \{k_i^R + k_i^D + \omega\}\theta_i(t) + \omega \sum_j P_{ij} \, \theta_j(t), \quad (32)$$

where $\theta_i(t) = \theta_p(E_i, t)$ and E_i is the energy of the ith grain. Equation (32) describes the rate of change of the population of the ith grain and is one of a linear system of nonhomogeneous, coupled differential equations that can be written more compactly in matrix form,

$$\frac{d\boldsymbol{\theta}(t)}{dt} = \mathbf{F}(t) + \{\omega(\mathbf{P} - \mathbf{I}) - \mathbf{k}^R - \mathbf{k}^D\}\boldsymbol{\theta}(t) = \mathbf{F}(t) + \mathbf{J}\boldsymbol{\theta}(t). \quad (33)$$

In Eq. (33), $\boldsymbol{\theta}(t)$ is the physisorbed complex population vector, $\mathbf{F}(t)$ is the incident flux vector, $\mathbf{k}^R$ and $\mathbf{k}^D$ are diagonal matrices containing the grained rate constants, and $\boldsymbol{P}$ is the energy transfer probability matrix.

To solve the Eq. (33) EGME in the general case we use the right eigenvector matrix $\mathbf{X}_R$ of the matrix $\boldsymbol{J}$ to diagonalize $\boldsymbol{J}$ via a similarity transformation,

$$\mathbf{X}_\mathbf{R}^{-1} \mathbf{J} \, \mathbf{X}_R = \boldsymbol{\Lambda}, \quad (34)$$

so that

$$\mathbf{J} = \mathbf{X}_\mathbf{R} \, \boldsymbol{\Lambda} \, \mathbf{X}_\mathbf{R}^{-1}, \quad (35)$$

where $\boldsymbol{\Lambda}$ is the diagonal matrix of the eigenvalues of $\boldsymbol{J}$. Substituting Eq. (35) into Eq. (33) and multiplying from the left by $\mathbf{X}_\mathbf{R}^{-1}$ gives

$$\frac{d}{dt}(\mathbf{X}_\mathbf{R}^{-1} \, \boldsymbol{\theta}(t)) = \mathbf{X}_\mathbf{R}^{-1} \, \mathbf{F}(t) + \boldsymbol{\Lambda}(\mathbf{X}_\mathbf{R}^{-1} \, \boldsymbol{\theta}(t)). \quad (36)$$

Rearranging and multiplying from the left by $\exp(-\boldsymbol{\Lambda}t)$ gives

$$e^{-\boldsymbol{\Lambda}t}\left\{ \frac{d}{dt}(\mathbf{X}_\mathbf{R}^{-1} \, \boldsymbol{\theta}(t)) - \boldsymbol{\Lambda} \, \mathbf{X}_\mathbf{R}^{-1} \, \boldsymbol{\theta}(t) \right\} = e^{-\boldsymbol{\Lambda}t}(\mathbf{X}_\mathbf{R}^{-1} \, \mathbf{F}(t)). \quad (37)$$

Equation (37) can now be integrated in time by noting that the bracketed expression on the left is just the time derivative of $\exp(-\boldsymbol{\Lambda}t) \, \mathbf{X}_\mathbf{R}^{-1} \, \boldsymbol{\theta}(t)$,

$$\int_0^t d\{e^{-\boldsymbol{\Lambda}t'} \, \mathbf{X}_\mathbf{R}^{-1} \, \boldsymbol{\theta}(t')\} = \int_0^t e^{-\boldsymbol{\Lambda}t'} \, \mathbf{X}_\mathbf{R}^{-1} \, \mathbf{F}(t')dt'. \quad (38)$$

Carrying out this integration we are left with a general solution for $\boldsymbol{\theta}(t)$ that only requires us to find the eigenvectors and eigenvalues of the $\boldsymbol{J}$ matrix

$$\boldsymbol{\theta}(t) = \mathbf{X_R}\ e^{\Lambda t}\ \mathbf{X_R^{-1}}\ \boldsymbol{\theta}(0) + \mathbf{X_R}\ e^{\Lambda t} \int_0^t e^{\Lambda t'}\ \mathbf{X_R^{-1}}\ \mathbf{F}(t')\ dt'.$$

$$(39)$$

To make further progress, an exact form for the incident flux $\mathbf{F}(t)$ must be specified. For example, the energetics of $\mathbf{F}(t) = F(E,t)$ for a molecular beam impinging on a surface are given by Eq. (7). By choosing $\mathbf{F}(t)$ to be a step function in time, the evolution of $\boldsymbol{\theta}(t)$ towards steady state can be observed. Let us emphasize the point that $F(E,t)$ can take on any form, both in energy and time, that experiment dictates.

With $\boldsymbol{\theta}(t) = \theta_p(E,t)$ in hand after solving Eq. (39), the time and energy dependencies of the reactive and desorptive fluxes can be calculated as

$$F_R(E,t) = k_R(E)\ \theta_p(E,t) \qquad (40)$$

and

$$F_D(E,t) = k_D(E)\ \theta_p(E,t), \qquad (41)$$

respectively. The experimentally realized sticking coefficient for a surface that has been exposed to an incident gas flux, $F(E,t)$, for a time t', is

$$S = \frac{\int_0^\infty \int_0^\infty k_R(E)\ \theta_p(E,t)\ dE\ dt}{\int_0^{t'} \int_0^\infty F(E,t)\ dE\ dt}. \qquad (42)$$

Finally, any solution, $\theta_p(E,t)$, of the Master equation must obey the conservation equation,

$$\int_0^\infty \int_0^\infty F(E,t)\ dE\ dt = \int_0^\infty \int_0^\infty (k_R(E) + k_D(E))$$
$$\times \theta_p(E,t)\ dE\ dt, \qquad (43)$$

expressing the fact that all particles incident on the surface must eventually desorb or react.

IV. APPLICATION TO $CH_{4(g)} \leftrightarrow CH_{3(c)} + H_{(c)}$ REACTIONS ON Pt(111)

Activated dissociative chemisorption of methane on Pt(111) is considered to be a direct process that occurs during the course of individual molecule–surface collision trajectories without trapping of the molecules and thermalization to the surface temperature. A trapping mediated reaction channel for CH_4 dissociative chemisorption is discounted by detailed balance arguments because the associative desorption of CH_4 from the 240 K thermal reaction of $H_{(c)} + CH_{3(c)}$ on Pt(111) displays a $\cos^{37}(\vartheta)$ angular distribution without any trace of a diffuse $\cos(\vartheta)$ component indicative of trapping and thermalization before desorption.[49] In addition, Madix and co-workers[50] have shown that the CH_4 trapping probability on Pt(111) at low temperatures (ca. 100 K) drops sufficiently rapidly as the translational energy is increased that trapping will be negligible at the higher CH_4 energies and surface temperatures to be considered here.

In Sec. IV A, the PC–MURT model is employed to calculate dissociative sticking coefficients appropriate for Luntz and co-workers' supersonic molecular beam measurements of methane dissociative sticking on Pt(111) as functions of

methane translational and vibrational energies, isotope, and surface temperature. Simulation of all the molecular beam data required adjustment of only three parameters: (1) the apparent threshold energy for CH_4 dissociation on Pt(111), (2) the lumped frequency of the CH_4-surface vibration and frustrated rotations in the physisorption potential well, and (3) the total number of surface vibrational oscillators that freely exchange energy within the physisorbed complex. Having established these parameters once and for all, the PC–MURT is then used to predict the methane dissociative sticking coefficient as a function of the nozzle temperature of the molecular beam.

Next, in Sec. IV B, the PC–MURT is used to simulate the thermal programmed desorption (TPD) spectrum of physisorbed CH_4 on Pt(111). Simulation of the TPD spectrum required adjustment of one additional parameter, the physisorption well depth, which is needed for implementation of the full Master equation (ME). In Sec. IV C, the PC–ME is implemented for the CH_4/Pt(111) system and used to calculate the steady state coverage of physisorption complexes, sticking coefficients, reactive and desorbing fluxes, and the time evolution of the coverage of physisorbed complexes. We find that energy transfer between the physisorbed complex and bulk platinum has only a small effect on the calculated dissociative sticking coefficients at the high energies of the CH_4/Pt(111) molecular beam experiments for physically reasonable choices of the two energy transfer parameters, α and ω. In Sec. IV D, the energy dependence of the density of states and time scales for reaction and desorption for the CH_4/Pt(111) physisorbed complexes are used to argue that a statistical description of this reactive system is reasonable. In Sec. IV E, the simpler PC–MURT is used with its three previously established parameters to calculate thermal dissociative sticking coefficients for CH_4 on Pt(111) as a function of temperature and isotope. Finally, in Sec. IV F, we derive both an exact and approximate form for the thermal activation energy.

A. Dissociative sticking of methane from a molecular beam

Supersonic molecular beams have been used to measure methane dissociative sticking coefficients on Pt(111) by separate groups at IBM,[30,51] Stanford,[52] and Finland[53] with distressingly variable quantitative results. The IBM data set is the most complete, has been quantitatively replicated in two separate molecular beam instruments at IBM, and has been the subject of previous theoretical simulations using a thermally assisted tunneling model[51] and an earlier implementation of our PC–MURT.[5] Here, we return to simulate the IBM data using a more computationally exact implementation of our PC–MURT with a different description of the desorption transition state and using the PC–ME approach outlined in Sec. III.

Dissociative sticking coefficients are readily calculated in a computationally exact manner using the simple PC–MURT of Eq. (29),

TABLE I. Normal mode vibrational frequencies, ν_i, and degeneracies, d_i, for gas phase CH_4 and CD_4 (Ref. 55).

Mode	CH_4 ν_i (cm^{-1})	CD_4 ν_i (cm^{-1})	d_i
1	2914	2085	1
2	1526	1054	2
3	3020	2258	3
4	1306	996	3

$$S = \int_0^\infty S(E^*)\, f(E^*)\, dE^*, \tag{29}$$

where $E^* = E - E_{ad}$. Two quantities are required to make such a calculation: the microcanonical sticking coefficient, $S(E^*)$, and the initial collision induced physisorbed complex energy distribution, $f(E^*)$. Microcanonical sticking coefficients were calculated from Eq. (27) using the Beyer–Swinehart state counting algorithm[54] for the transition states' sums of states. The initial energy distribution of the physisorbed complexes was calculated from Eqs. (8) and (28) via direct convolution of the independent canonical energy distributions of the various active degrees of freedom of the complexes. Finally, Eq. (29) was used to average the microcanonical sticking coefficient over the probability of forming a physisorbed complex at E^* to predict experimental dissociative sticking coefficients. However, prior to any of these calculations we must first specify what degrees of freedom of the physisorption complex are active and can freely exchange energy with one another on timescales short compared to the reactions, either desorption or dissociation.

Let us assume that each methane/Pt(111) physisorbed complex has ϕ degrees of freedom which actively exchange energy. The active degrees of freedom will be taken to include the nine internal vibrational modes of the molecule, the vibration along the surface normal and three modes of frustrated rotation of methane in the physisorption potential well, and s vibrational modes of the local cluster of surface atoms, such that $\phi = 13 + s$. Molecular translations in the plane of the surface are considered to be inactive modes because the experimentally measured dissociative sticking coefficient scales with the normal translational energy of the incident molecules. The frustrated rotations and normal vibration of the molecule in the physisorption potential well will be treated as external vibrational modes. All four of these external modes will be grouped together and considered to have equal vibrational frequencies, ν_D. The local cluster of surface atoms will be characterized by s active vibrational modes all sharing the mean frequency of the metal phonons in the Debye model ($\nu_s = \frac{3}{4} k_b T_{Debye}/h$, $T_{Debye} = 234$ K for bulk platinum). In the absence of definitive guidance from electronic structure calculations, the internal vibrational modes of methane in the collision complex are assumed to be the same as those of the gas phase molecule described by the frequencies ν_i and degeneracies d_i given in Table I for both CH_4 and CD_4.

The initial energy distribution of surface collision complexes, $f(E^*)$, is obtained by substitution of Eq. (8) into Eq. (28),

$$f(E^*) = \int_0^{E^*} f_t(E_t) \int_0^{E^* - E_t} f_s(E_s) \int_0^{E^* - E_s - E_t} f_v(E_v)$$

$$\times f_r(E^* - E_t - E_s - E_v)\, dE_v\, dE_s\, dE_t. \tag{44}$$

This distribution can be formed once the initial energy distributions for all $\phi = 13 + s$ active degrees of freedom contributing to the total energy of the complexes have been specified. These initial distributions are assumed to be independent and include distributions for the normal translational motion, the three rotational degrees of freedom, and the nine vibrational modes of the methane incident from the molecular beam, as well as the distribution for the s oscillators of the local cluster of surface atoms. As previously noted, each group of modes will be characterized by its own separate temperature in a molecular beam experiment.

The normalized flux weighted translational energy distribution for molecules in a supersonic molecular beam is[8,17]

$$f_t(E_t) = N E_t \exp\left(-\frac{(\sqrt{E_t} - \sqrt{E_b})^2}{k_b T_t}\right), \tag{45}$$

$$N = \frac{1}{(k_b T_t)^2}\left\{(\delta^2 + 1)e^{-\delta^2} + \sqrt{\pi}\left(\delta^3 + \frac{3}{2}\,\delta\right)\right.$$

$$\left. \times [1 + \mathrm{erf}(\delta)]\right\}^{-1}, \tag{46}$$

where E_b defines the stream energy of the beam, T_t is the translational temperature of the beam, N is a normalization constant, and $\delta = \sqrt{E_b/k_b T_t}$. Both E_b and T_t depend on the nozzle temperature and any carrier gas seeding. The translational temperature of the beam describes the width of the distribution and is typically much less than the nozzle temperature, T_n. In the simulations of the IBM molecular beam sticking data presented here, for which no T_t's are reported, we take $T_t = 25$ K as a reasonable estimate of the translational temperature of the beam.[17] Note that although E_b is not equal to the mean translational energy, they are approximately the same ($\langle E_t \rangle = E_b \pm 3\%$) for the molecular beams of the experiments discussed here.

The rotational energy distribution of molecules in the molecular beam can be described by the canonical distribution,

$$f_r(E_r) = \frac{\rho_r(E_r)}{Q_r}\,\exp\left(-\frac{E_r}{k_b T_r}\right), \tag{47}$$

where T_r is the rotational temperature, $\rho_r(E_r)$ is the rotational density of states, and Q_r is the rotational partition function. The rotational temperature is dependent on the molecular beam expansion conditions and is typically much less than the nozzle temperature. For example, the rotational temperature of methane in supersonic molecular beams has been estimated as $T_r \simeq 0.1\, T_n$.[52] While a quantum mechanical description of methane rotations is preferable, even for such a simple molecule as methane, implementing an exact state counting that fulfills nuclear statistics restrictions is cumbersome. Fortunately, the rotational levels of methane are sufficiently closely spaced[55] (the rotational constant B is 5.25 cm^{-1} for CH_4 and 2.65 cm^{-1} for CD_4) that even at the

low rotational temperatures typical of a molecular beam ($T_r \sim 50$ K) a classical description will be an adequate approximation for our purposes. For these reasons we model the rotations of methane as those of a classical spherical top, for which the density of states and partition function are[13]

$$\rho_r(E_r) = \frac{1}{\sigma} \frac{2\sqrt{E_r}}{B^{3/2}}, \tag{48}$$

$$Q_r = \frac{\sqrt{\pi}}{\sigma} \left(\frac{k_b T_r}{B} \right)^{3/2}, \tag{49}$$

where the symmetry number σ has been included to compensate for an over counting of rotational states in the classical phase space integral ($\sigma = 12$ for methane). The classical normalized canonical distribution for the three rotational degrees of freedom of methane is then

$$f_r(E_r) = \frac{\sqrt{E_r}}{\Gamma\left(\frac{3}{2}\right)(kT_r)^{3/2}} \exp\left(-\frac{E_r}{k_b T_r} \right), \tag{50}$$

where $\Gamma(x)$ is the gamma function. Note that while the symmetry number does not appear in the canonical distribution due to cancellation it is important to include it when calculating sums and densities of states for use in RRKM rate constants and in Master equation calculations.

The vibrational energy distribution of methane molecules incident on the surface with a common vibrational temperature, T_v, characteristic of the molecular beam is

$$f_v(E_v) = \frac{\rho_v(E_v)}{Q_v} \exp\left(-\frac{E_v}{k_b T_v} \right), \tag{51}$$

where $\rho_v(E_v)$ is the vibrational density of states and Q_v is the vibrational partition function. The vibrational density of states is calculated from the normal mode frequencies of methane using the Beyer–Swinehart algorithm. The vibrational temperature is usually assumed to be equal to the nozzle temperature of the molecular beam, although this correspondence may not always be valid as will be discussed later.

Finally, for the vibrational energy distribution of the local cluster of surface oscillators at temperature T_s that become involved in the physisorbed complex we use the canonical distribution

$$f_s(E_s) = \frac{\rho_s(E_s)}{Q_s} \exp\left(-\frac{E_s}{k_b T_s} \right). \tag{52}$$

The vibrational density of states, $\rho_s(E_s)$ of the local cluster of surface oscillators is calculated using the Beyer–Swinehart algorithm and is characterized by s surface vibrational modes of frequency $\nu_s = \frac{3}{4} k_b T_{\text{Debye}}/h$, as described above.

Figure 2 provides a representative example of the physisorbed complex $f(E^*)$ and its assembly by convolution from the distributions $f_s(E_s)$, $f_v(E_v)$, $f_r(E_r)$, and $f_t(E_t)$ appropriate for a molecular beam of CH_4 impinging on a Pt(111) surface under sufficiently energetic experimental conditions that the measured dissociative sticking coefficient is $S \sim 10^{-2}$.

In the absence of definitive guidance from electronic structure calculations, and in the spirit of developing a surface kinetics theory with a minimum number of adjustable parameters, we assume the transition states for dissociation and desorption are loose and share as many common mode frequencies with the physisorbed complex as possible. The dissociation transition state is characterized by ($\phi - 1$) active vibrational modes identical to those of the physisorbed complex with one of the ν_3 triply degenerate antisymmetric C–H stretch vibrations sacrificed as the reaction coordinate. The desorption transition state is taken as the isolated molecule far from the surface where the rotational motion of the gas phase molecule is fully developed. Consequently, the desorption transition state is characterized by ($\phi - 4$) active vibrational modes identical to those of the physisorbed complex, where the normal vibrational mode is the reaction coordinate, and the three frustrated rotational modes of the physisorbed complex have evolved into rotations of the free molecule. Here again, we treat the methane rotations as those of a classical spherical top whose sum of states is[13]

$$W_r(E_r) = \frac{4}{3} \frac{1}{\sigma} \left(\frac{E_r}{B} \right)^{3/2}. \tag{53}$$

Using these parameters along with the vibrational frequencies given above it is possible to evaluate the microcanonical sticking coefficient of Eq. (27),

$$S(E^*) = \frac{W_R^{\ddagger}(E^* - E_0)}{W_R^{\ddagger}(E^* - E_0) + W_D^{\ddagger}(E^*)}, \tag{27}$$

using the Beyer–Swinehart state counting algorithm.

Having specified the quantities required to make a dissociative sticking coefficient calculation for molecules incident from a molecular beam it should be clear that there are just three adjustable parameters: (1) the apparent threshold energy for dissociative chemisorption, E_0 (see Fig. 1), (2) the lumped vibrational frequency representative of the normal vibration and frustrated rotations of the molecule in the physisorption potential well, ν_D, and (3) the number of active surface oscillators, s. All other variables in the PC–MURT are fixed by either experimental conditions or preexisting and physically reasonable assumptions. Clearly, a more flexible and parameter rich theory is possible if all the mode frequencies of the physisorbed complex and desorption and dissociation transition states are allowed to independently vary. Fortunately, this is largely unnecessary based on the assumptions discussed above. In the future, EST should be able to supply all these mode frequencies and threshold energies directly.

The dissociative sticking coefficient observed in supersonic molecular beam experiments may now be calculated using Eq. (29) to perform the averaging of the microcanonical sticking coefficient over the physisorbed complex energy distribution. This direct method for calculating the sticking coefficient can be easily handled by current desktop computers with most calculations taking only a few minutes to complete.

Figure 3 compares PC–MURT simulations using the above expressions with the Luntz and Bethune molecular
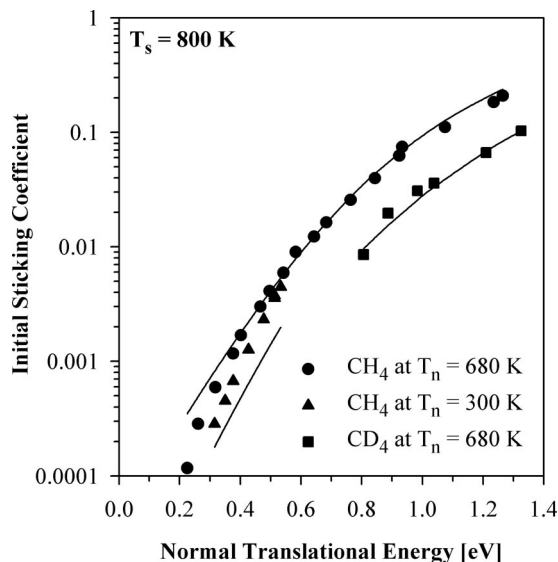
FIG. 3. Comparison of theoretical simulations for methane dissociative sticking on Pt(111) as a function of normal translational energy with data points from molecular beam experiments (Refs. 30 and 51).

FIG. 4. Comparison of theoretical simulations of CH_4 dissociative sticking on Pt(111) as a function of surface temperature for various normal translational energies with data points from molecular beam experiments (Refs. 30 and 51).

beam experimental data[30,51] for CH_4 taken at $T_n = 680$ and 300 K, and for CD_4 taken at $T_n = 680$ K. In all experiments the surface temperature was held at 800 K. Following Madix,[52] the vibrational temperature of the molecules was taken to be equal to the nozzle temperature, $T_v = T_n$, and the rotational temperature was estimated as $T_r = 0.1 T_n$. These data were used to fix the three adjustable parameters of the PC–MURT by grid searching the associated three dimensional parameter space for a global minimum in the average relative discrepancy between simulation and experiment, assuming equal weighting for all measurements. Best overall agreement with all three sets of molecular beam experimental data was achieved for CH_4/Pt(111) parameters of $E_0 = 0.61$ eV, $\nu_D = 110$ cm^{-1}, and $s = 3$. The CH_4/Pt(111) parameters uniquely fix those appropriate for CD_4/Pt(111) as $E_0 = 0.655$ eV, $\nu_D = 95$ cm^{-1}, and $s = 3$. The main effect of perdeuteration is to increase the reaction barrier height by the difference in the zero point energies of the C–H(D) reaction coordinate, 0.045 eV. This primary isotope effect suffices to explain the kinetic isotope effect observed in Fig. 3. There is no experimental evidence to suggest that tunneling of hydrogen across the barrier is significant. The worsening agreement between theory and experiment as the normal translational energy decreases in Fig. 3 is believed to be related to increasing vibrational cooling in the molecular beam as the gas seeding mixture is varied to obtain slower beams (*vide infra*).

Having once fixed the three parameters of the statistical model by fitting the $S(E_n,T_s = 800$ K$)$ experimental molecular beam data it is possible to calculate dissociative sticking coefficients for any other set of experimental conditions. Figure 4 presents simulations of the dissociative sticking coefficient as a function of surface temperature, $S(T_s;E_n,T_n = 680$ K$)$, for several normal translational energies. These simulations used no adjustable parameters and quite faithfully reproduce the experimental results.
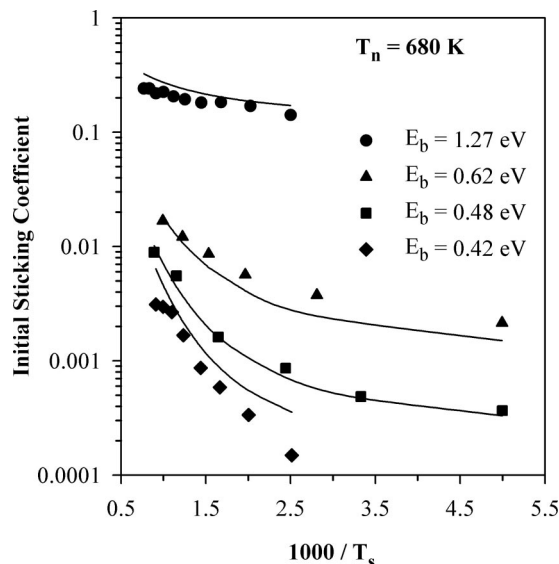
Although no experimental data have been published on the dissociative sticking coefficient of CH_4 on Pt(111) as a function of nozzle temperature, $S(T_n;E_n,T_s)$, we have simulated this dependence using the parameters fixed by simulation of the $S(E_n,T_s = 800$ K$)$ data. These results are presented in Fig. 5 for several normal translational energies at a surface temperature of 800 K. These simulations show the same qualitative behavior with varying T_n as did experimental molecular beam data for methane sticking on Ni(100).[8,17]

An important point to be noted from Figs. 4 and 5, that are plotted in "Arrhenius style," is that the slope of the curves vary markedly with the beam translational energy and although each slope might be related to an "effective activation energy" characteristic of the experimental specifics,
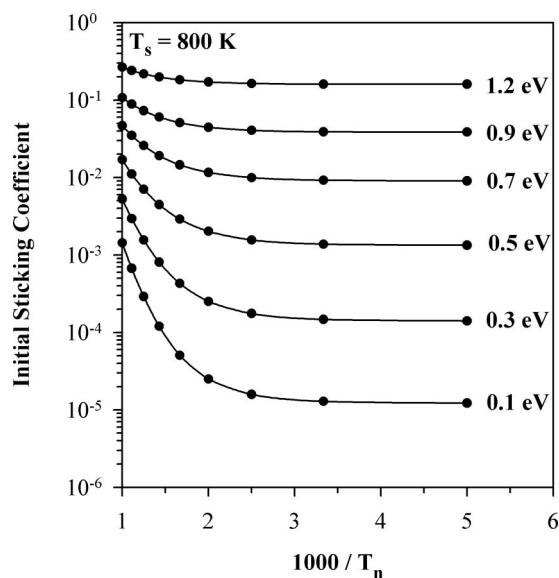

FIG. 5. Theoretical predictions of CH_4 dissociative sticking on Pt(111) as a function of nozzle temperature for various normal translational energies.

none can be individually ascribed to the overall activation energy, E_a, or the apparent threshold energy for dissociation, E_0, characteristic of the reactive multidimensional potential energy surface.

B. Desorption energy from thermal programmed desorption

The thermal programmed desorption (TPD) spectrum of physisorbed methane on Pt(111) has been measured in our laboratory and shows that methane desorbs at 65 K with a best fit desorption energy of 0.221 eV and a pre-exponential of 1×10^{17} s^{-1}. Here we simulate this TPD spectrum using the PC–MURT to extract the desorption energy of the CH_4/Pt(111) system. The full Master equation could also be used for this simulation but given the success of the simpler PC–MURT with the molecular beam data we have chosen it instead.

Under the assumption that the adsorbates are maintained in thermal equilibrium with the surface during TPD, simulation of the TPD spectrum requires calculation of the thermal rate constant for desorption and solution of a differential equation governing the temperature dependence of the methane coverage. Following Baer and Hase,[13] the thermal rate constant for desorption, $k_D(T)$, is obtained by averaging the microcanonical rate constant for desorption, $k_D(E)$, over the thermal energy distribution of physisorbed complexes, $f_T(E)$,

$$k_D(T) = \int_0^\infty k_D(E) \, f_T(E) \, dE. \tag{54}$$

The thermal energy distribution of the physisorbed complexes is given by

$$f_T(E) = \frac{\rho(E)}{Q(T)} \exp\left(-\frac{E}{k_b T}\right), \tag{55}$$

where $\rho(E)$ is the density of states obtained from convolution of the independent densities of states of all active degrees of freedom of the physisorbed complex and $Q(T)$ is the associated partition function. Within the PC–MURT framework, the microcanonical rate constant for desorption is given by RRKM theory as

$$k_D(E) = \frac{W_D^\ddagger(E - E_D)}{h \, \rho(E)}, \tag{56}$$

where $W_D^\ddagger(E - E_D)$ is the sum of states at the transition state for desorption. Substitution of Eqs. (55) and (56) into Eq. (54), followed by the change of variables $E^* = E - E_D$ yields a simplified expression for the thermal rate constant,

$$k_D(T) = \frac{e^{-E_D/k_b T}}{h \, Q(T)} \int_0^\infty W_D^\ddagger(E^*) \exp\left(-\frac{E^*}{k_b T}\right) dE^*. \tag{57}$$

The integral in Eq. (57) can be integrated by parts to give the partition function of the desorption transition state, $Q_D^\ddagger(T)$, times $k_b T$. The result of this derivation is the canonical transition state theory (TST) expression for the thermal rate constant,
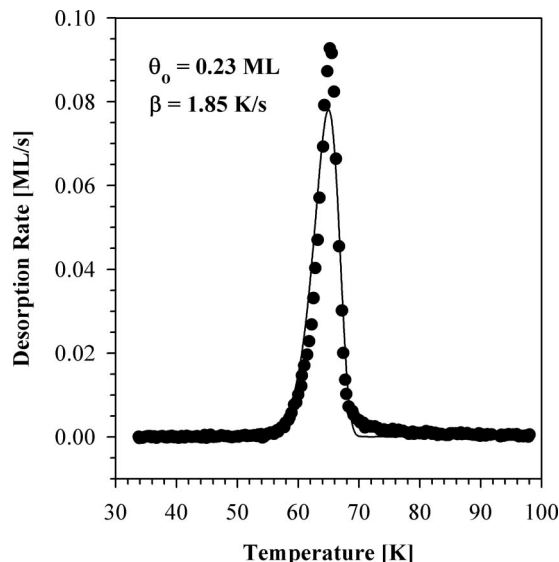

FIG. 6. PC–MURT simulation of an experimental thermal desorption spectrum for 0.23 ML CH_4 on Pt(111). The statistical model gives a pre-exponential factor of 3.5×10^{12} s^{-1} and a desorption barrier height of $E_D = 0.163$ eV (cf. $k_b T/h$ at 65 K $\approx 1.4 \times 10^{12}$ s^{-1}).

$$k_D(T) = \frac{k_b T}{h} \frac{Q_D^\ddagger(T)}{Q(T)} \exp\left(-\frac{E_D}{k_b T}\right) = A(T) \exp\left(-\frac{E_D}{k_b T}\right). \tag{58}$$

The temperature dependent pre-exponential of Eq. (58), $A(T)$, is readily calculated given the active degrees of freedom of the physisorbed complex and the reaction coordinate for desorption described in Sec. IV A,

$$A(T) = \frac{k_b T}{h} \frac{Q_D^\ddagger(T)}{Q(T)} = \frac{k_b T}{h} \frac{Q_{rot}^{CH_4}(T)}{Q_{vib}^{ext}(T)}, \tag{59}$$

where $Q_{rot}^{CH_4}(T)$ and $Q_{vib}^{ext}(T)$ are the partition functions for rotational motion of gas phase methane and for the four grouped external vibrational modes of the physisorbed complex, respectively. Evaluation of Eq. (59) yields a canonical TST pre-exponential of 3.5×10^{12} s^{-1} at 65 K. This pre-exponential is about twice what one would expect for a unimolecular reaction in which the reactant very closely resembles the transition state (i.e., $k_b T/h$ at 65 K $\approx 1.4 \times 10^{12}$ s^{-1}).

With expressions (58) and (59) for the thermal rate constant for desorption, the methane desorption rate in the TPD spectrum is given by

$$\frac{d\theta(T)}{dT} = -\frac{1}{\beta} k_D(T) \, \theta(T) = -\frac{A(T)}{\beta} e^{-E_D/k_b T} \, \theta(T), \tag{60}$$

where E_D is the desorption energy, β is the linear heating rate, and $\theta(T)$ is the methane coverage. Figure 6 shows the experimental and simulated TPD spectra of physisorbed methane on Pt(111). By forcing the peak desorption temperature in the simulation to match the 65 K experimental value, the desorption energy is fixed as $E_D = 0.163$ eV.

C. Time evolution of the energy distribution of the physisorbed complexes

In addition to the simple PC–MURT, the full PC–ME for the time evolution of the coverage of physisorbed complexes, Eq. (22), can also be used to simulate dissociative sticking coefficients. As demonstrated earlier in this section, the PC–MURT without vibrational energy transfer enjoys both qualitative and quantitative success in simulations of methane dissociative sticking coefficients on Pt(111) as functions of normal translational energy, surface temperature, and isotope. In addition, the PC–MURT was used to find the desorption energy of the CH_4/Pt(111) system by simulation of the TPD spectrum of physisorbed methane on Pt(111). In treating the methane TPD, the PC–MURT was shown to naturally recover the appropriate canonical transition state theory for CH_4 thermal desorption. Nonetheless, it remains to be shown whether vibrational energy transfer between the physisorbed complex and the bulk platinum can be safely neglected in models of methane dissociative chemisorption.

Implementation of the full PC–ME for the CH_4/Pt(111) system requires specification of three additional parameters over those needed to implement the PC–MURT: (1) the desorption energy, E_D, (2) the inelastic collision frequency, ω, and (3) the parameter α of the collision step-size distribution within the density-weighted exponential down model [see Eq. (16)]. The desorption energy was determined in Sec. IV B by simulation of the TPD spectrum of physisorbed methane on Pt(111) to be 0.163 eV, and this is the value used in all Master equation simulations presented here. The parameters α and ω, while in principle fully adjustable, must be chosen to be physically realistic. As described earlier, we assume that vibrational energy transfer is a phonon mediated process and take ω to be the three times the mean phonon frequency, 1.1×10^{13} s^{-1}, and α equal to the mean phonon energy, 122 cm^{-1}, of Pt. Recall that α is a good estimate of the average energy transferred in downward inelastic collisions, $\langle \Delta E(E') \rangle_d$ of Eq. (20). Finally, all PC–ME simulation results presented here use the PC–MURT parameters determined in Sec. IV A from fitting the molecular beam experimental data; for CH_4 these are $E_0 = 0.61$ eV, $\nu_D = 110$ cm^{-1}, and $s = 3$.

For comparison with experimental dissociative sticking coefficient measurements, the Eq. (22) Master equation must be solved for the steady state distribution of physisorbed complexes, $\theta_p^{ss}(E)$. Following Eq. (42), the steady state sticking coefficient is given as

$$S^{ss} = \frac{1}{F_0} \int_0^\infty k_R(E) \; \theta_p^{ss}(E) \; dE. \tag{61}$$

The steady state reactive flux, desorbing flux, and conservation equation are defined in analogy to their time dependent counterparts, see Eqs. (40), (41), and (43), but with the time dependence dropped.

Using the CH_4/Pt(111) parameters defined above, we have simulated the dissociative sticking coefficient of methane on Pt(111) using the Master equation. These results are shown for the $S(E_n; T_s = 800$ K, $T_n = 680$ K) data in Fig. 7 along with the best fit PC–MURT result (dashed curve) from
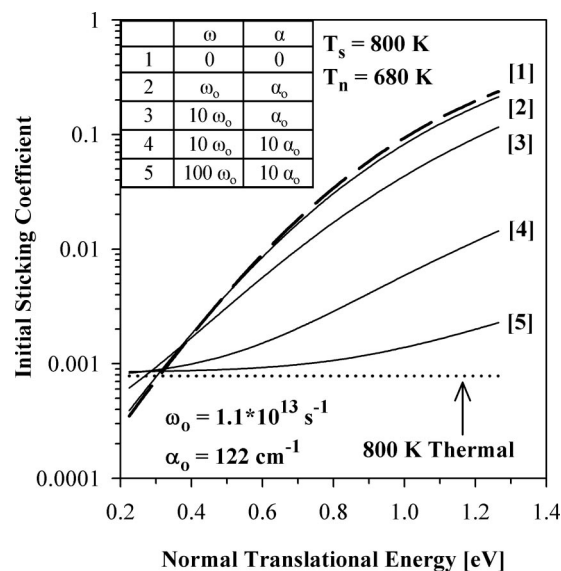

FIG. 7. Master equation simulations of CH_4 dissociative sticking coefficients on Pt(111) as a function of normal translational energy for various choices of the inelastic collision frequency ω and the α parameter of the density-weighted exponential down model of the collision step-size distribution. The dashed curve is the best fit PC–MURT simulation of Fig. 3 and the dotted line is the predicted 800 K thermal sticking coefficient for an ambient $CH_{4(g)}$/Pt(111) system at thermal equilibrium.

Sec. IV A and the predicted 800 K thermal sticking coefficient (dotted line) from Sec. IV E. The second curve in Fig. 7 gives the PC–ME predicted sticking coefficient for our base choices of ω and α, as indicated in the figure. These simulations show that inclusion of energy transfer has only a small effect ($\pm 10\%$ at most) on sticking coefficients calculated with the simple PC–MURT for this system. Furthermore, as the energy transfer parameters are increased, the sticking coefficient at all normal translational energies approaches the sticking value for a system at thermal equilibrium at the temperature of the 800 K surface. In this particular simulation, inclusion of energy transfer leads to increased sticking at low translational energies and decreased sticking at high translational energies. The general effect of energy transfer on these types of nonthermal systems is always to shift nonthermal distributions towards a thermal distribution at the surface temperature. With sufficiently high energy transfer, it is always possible to attain the thermal sticking coefficient appropriate to an equilibrium system at the surface temperature.

Typical collision step-size distributions, $P(E, E')$, at reaction threshold for the density weighted exponential down model are plotted in Figs. 8(a) and 8(b) as functions of α and surface temperature, respectively. The elastic energy transfer peak has been excluded from these plots since it is not necessary to include it in the energy grained Master equation Eq. (32). Figure 8(a) shows $P(E, E')$ at the 800 K surface temperature of the molecular beam $S(E_n)$ experiments as a function of α. Due to the relatively high surface temperature, detailed balance [see Eqs. (16) and (17)] insures that these distributions are fairly symmetrical about the elastic peak, while α controls the overall width of the distributions. In contrast, Fig. 8(b) shows that at fixed α, lowering the surface temperature skews the distribution towards

(a)

(b)
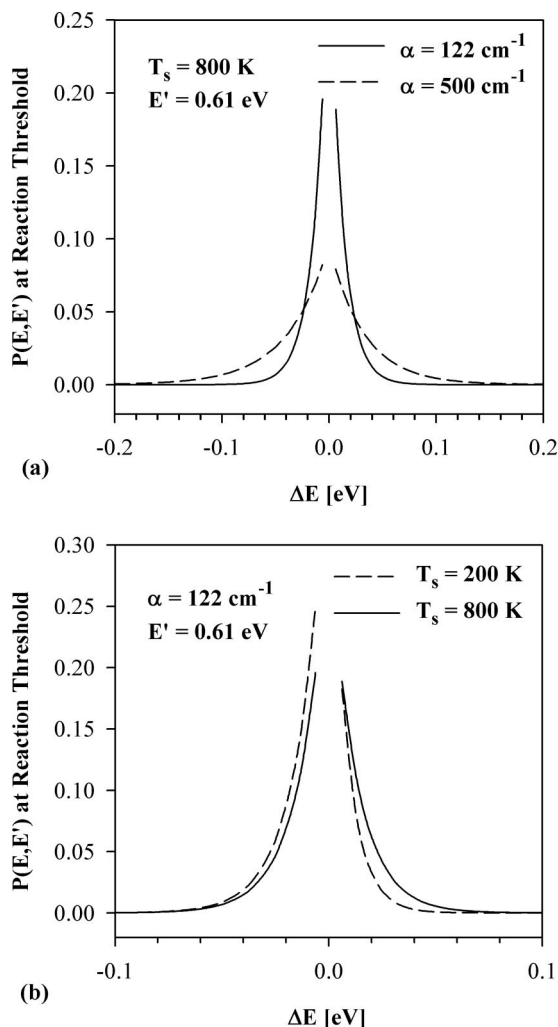
FIG. 8. Sample collision step size distributions for the density weighted exponential down model at reaction threshold as (a) a function of α at 800 K surface temperature and (b) as a function of surface temperature at $\alpha = 122$ cm^{-1}.

FIG. 9. Various energy probability distributions at reaction threshold for the CH$_4$ on Pt(111) system. (a) The physisorbed complex distribution formed collisionally by the incident beam when the beam stream energy is at the reaction threshold [cf. $f(E^*)$ of Fig. 2]. (b) The steady state distribution of physisorbed complexes. (c) The distribution of physisorbed complexes appropriate to thermal equilibrium at $T_s = 800$ K.

downward energy transfer, in agreement with detailed balance. Note that product terms of the form $R(E,E')\theta_p(E') = \omega P(E,E')\theta_p(E')$ ultimately dictate the vibrational energy transfer between the physisorbed complexes and metal within the PC–ME of Eqs. (5) and (22). Under nonequilibrium conditions, the sticking coefficient tends towards its thermal value at the surface temperature and the overall vibrational energy transfer is downwards for hyperthermal $F(E,t)$ distributions and upwards for hypothermal distributions.

Figure 9 compares the incident, steady state, and thermal distributions of the physisorbed complexes at reaction threshold for the CH$_4$/Pt(111) system. Clearly, relaxation of the incident distribution towards the thermal distribution at steady state is far from complete. In addition, there is very little difference between the incident and steady state distributions in their high energy tails indicating that relaxation of the incident distribution takes place primarily at the expense of population at and below the mean energy of the distribution. Notice that at the high E' and T_s of Fig. 8(a) the $P(E,E')$ distribution is fairly symmetric around zero energy
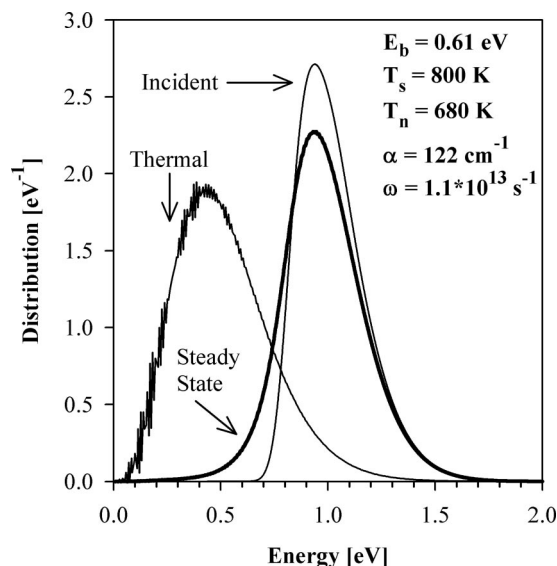
transfer. Overall, for the relatively high energy physisorbed complex distribution of Fig. 9 there is no net uptake of energy from the surface by the physisorbed complex. This is because the ''effective temperature'' of the initial physisorbed complex distribution [i.e., $f(E)$] is greater than the 800 K surface temperature. If the ''temperature'' of the physisorbed complex was less than 800 K, there would be a net energy transfer to the complex via detailed balance.

Having illustrated the effect of vibrational energy transfer on the distribution of physisorbed complexes that goes on to react or desorb, Fig. 10 shows the steady state distribution and the associated reactive and desorbing flux distributions at reaction threshold. Note that because dissociative chemi-
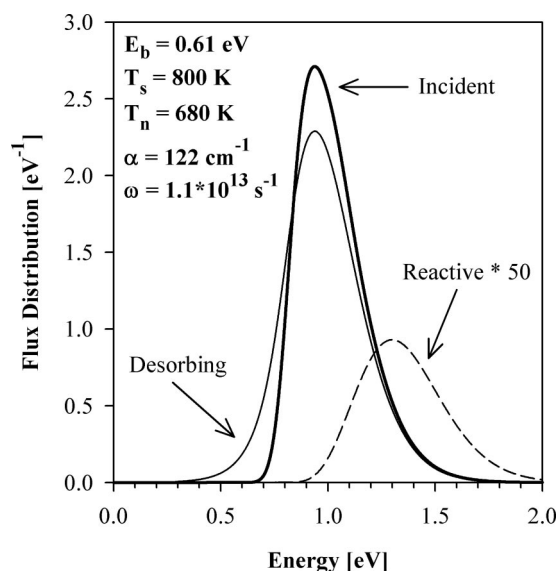

FIG. 10. Steady state flux distributions for CH$_4$ on Pt(111). (a) The incident flux of physisorbed complexes created, normalized to unity. (b) The desorbing flux distribution. (c) The reactive flux distribution multiplied by 50.
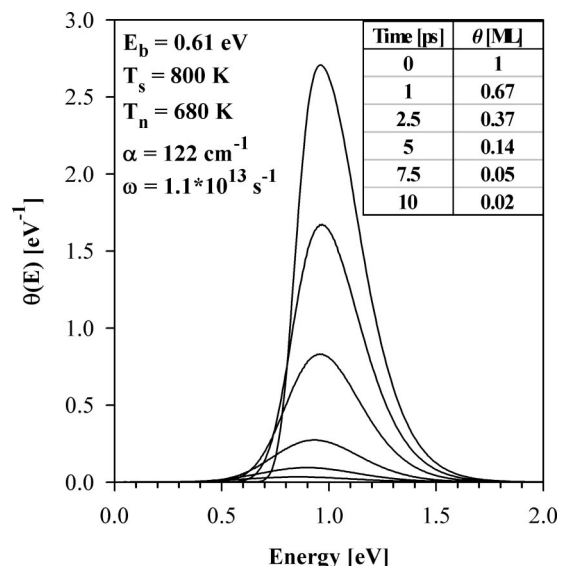
FIG. 11. Time evolution of the coverage of physisorbed complexes for CH_4 incident on Pt(111) near the reaction threshold for an incident distribution that is a delta function in time.

sorption is a rare event under the reaction conditions of Fig. 10 ($S \sim 10^{-2}$), the reactive flux in Fig. 10 has been multiplied by 50 to make it visible on the scale of the desorbing flux. Clearly, the vast majority of the steady state flux desorbs and it is only the high energy portion that has any chance of reacting. Given that there is very little energy relaxation between the incident and steady state physisorbed complex distributions and that it is the overlap of the microcanonical sticking coefficient and the distribution of physisorbed complexes above the barrier to reaction that results in a nonzero contribution to the sticking coefficient, the small effect of energy transfer on this system's overall sticking coefficient is reasonable.

In addition to solving the Master equation at steady state to obtain dissociative sticking coefficients, it is also possible to examine the time evolution of the coverage of physisorbed complexes, $\theta_p(E,t)$, for arbitrary incident flux, $F(E,t)$. An example of this type of calculation is given in Fig. 11 for the CH_4/Pt(111) system. For this simulation the incident flux energy distribution was taken to be that from a molecular beam with the temporal dependence taken as a delta function, $F(E,t) = F_0 f(E) \delta(t)$. The small amount of downward energy transfer occurring in this system is clearly illustrated by the modest downward movement of the low energy tail of the physisorbed complex distribution as time progresses.

In the absence of tunneling through the reaction barrier, classical transition state theory provides an upper bound for the rate constant of a reaction with fixed transition state characteristics due to the fundamental assumption of direct dynamics with no barrier recrossings. In analogy with transition state theory, and taking into account the effects of vibrational energy transfer as included in the Master equation, dissociative sticking coefficients calculated from our PC–MURT should also provide an upper bound on the sticking coefficient at hyperthermal energies. Note that at high energy, where the initial physisorbed complex distribution is hyperthermal, the net energy relaxation will always be in the

downwards direction. The PC–MURT, which neglects this effect, will provide an upper bound on the sticking. In addition, the calculated sticking coefficient is most sensitive to the apparent reaction threshold energy in the high energy regime. *Consequently, by fitting hyperthermal experimental data (subject to downwards energy relaxation), the PC–MURT determined apparent reaction threshold energy provides an upper bound on the true E_0.*

Finally, it is instructive to note that in the limit of large substrate atom separation the microcanonical unimolecular rate theory presented here goes over smoothly to the gas phase kinetics of a long-lived bimolecular collision complex that can collisionally exchange energy with an ambient gas. The PC–MURT has been formulated in analogy with gas phase kinetics through the idea of a localized adsorbate/substrate "physisorbed complex." Given the success of statistical theories of reaction rates and Master equation treatments of vibrational energy transfer in the gas phase,[33,34] we anticipate that these theories should also enjoy some measure of success when applied at the gas–solid interface.

D. Reaction time scale issues

A recurring question in the discussion of surface reactions is whether a statistical theory can be adequate for a quantitative description of the kinetics or must a full dynamical theory be employed. Unfortunately, unless a statistical treatment is feasible it is unlikely that rigorous kinetics calculations for high dimensionality surface reactions will ever be computationally tractable. In the gas phase, formal applicability of microcanonical RRKM rate theory usually relies on two criteria being met:[56] (a) the energized reactants at energy E should act as if they are distributed microcanonically and react with a single rate constant, $k(E)$, independent of quantum state, and (b) intramolecular vibrational energy redistribution (IVR) should be faster than any reaction rate in order to maintain the microcanonical distribution over the course of the reaction. After applying the PC–MURT and PC–ME to the dissociative chemisorption of the methane molecular beams on Pt(111), let us return to more critically consider whether these RRKM applicability criteria can be consistently satisfied for the surface reactions.

For isolated molecules in the gas phase,[57,58] IVR does not typically begin until energies are reached for which the molecular state density, $\rho(E)$, exceeds $10-100$ states/cm^{-1}. For molecules at energies above this threshold state density, IVR rates are in the range from 10^8 -10^{13} s^{-1}. Although IVR rates tend to increase with state density for a given molecular species, the rates are generally not predictable across a series of structurally different molecules[57] except after detailed theoretical modeling.[59] The vibrational state density calculated via the Beyer–Swinehart algorithm for the CH_4/Pt(111) physisorbed complexes as a function of total energy measured from the bottom of the physisorption well is presented in Fig. 12. The PC state density at reactive energies, $E \geqslant 0.77$ eV, is greater than 10^6 states/cm^{-1}, well above the threshold for the onset of IVR. The state density includes contributions from the nine relatively high frequency vibrational modes of methane, the four 110 cm^{-1} modes of the molecule moving within the
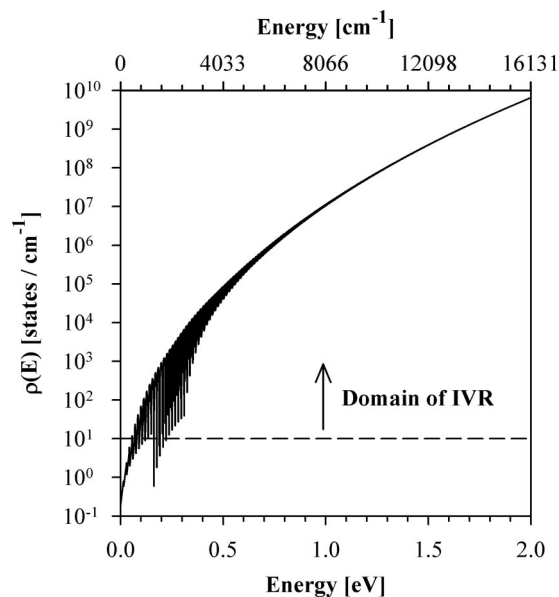
J. Chem. Phys., Vol. 118, No. 2, 8 January 2003

Microcanonical unimolecular rate theory   859

FIG. 12. Physisorbed complex density of states as a function of total active energy E for CH_4 interacting with Pt(111). At reactive energies ($E \geq 0.77$ eV), the density of states is greater than 10^6 states per cm^{-1}.

FIG. 13. Unimolecular time constants $[k(E)^{-1}]$ for desorption and reaction for CH_4 on Pt(111). At reactive energies the time constant for desorption is 2.7 ps. The microcanonical sticking coefficient, $S(E) = \tau_D(E)/[\tau_D(E) + \tau_R(E)]$, is plotted on a linear scale.

physisorption well, and the three 122 cm^{-1} modes of the Pt surface oscillators. Quack has shown that IVR between the C–H stretch and bending modes of gas phase methane is rapid and occurs on a 100–500 fs time scale, as is also the case for various halomethanes.[60] The IVR lifetime of methylene iodide (CH_2I_2) was experimentally measured in solution to be 9–10 ps after fs optical excitation to an energy of 0.6 eV.[61] Interestingly, this molecule shares some of the high and low frequencies of the CH_4/Pt(111) physisorbed complex modes, with the lowest frequency mode being the CI_2 bend at 121 cm^{-1}. Theoretical analysis of the CH_2I_2 IVR found that microcanonical equilibration of the higher frequency C–H modes was complete on a sub-ps to ps time scale but that energy flow to the lower frequency CI_2 modes was more weakly coupled and took somewhat longer (6–9 ps).[62] With the larger number of low frequency modes and higher state densities for the surface PC at reactive energies, it is not unreasonable to speculate that IVR rates for potentially reactive PCs will occur on a sub-ps to few ps time scale. Unfortunately, most spectroscopic investigations and accumulation of theoretical wisdom on IVR rates have involved studies of molecules at energies insufficient to break or rearrange covalent bonds. It is precisely at these higher reactive energies, where the molecular potential becomes softened and distorted in the region of the transition state, that anharmonic cross couplings between vibrational modes should be rapidly increasing and as the agent of IVR these couplings should markedly increase IVR rates. Many years ago, Rabinovitch concluded that IVR normally completes on a subpicosecond time scale for the overwhelming majority of hydrocarbon reactions at reactive energies based on adherence to RRKM kinetics at high gas pressures.[63] More recently, laser studies of the unimolecular decomposition of isolated small molecules in the gas phase have largely shown quantum state resolved adherence to RRKM kinetics despite
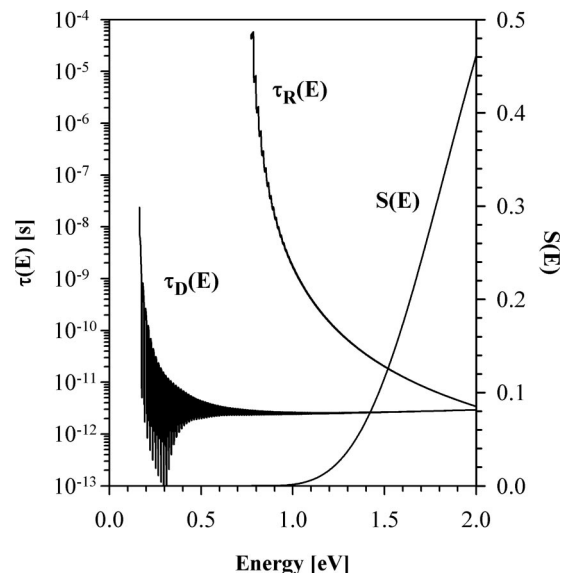
relatively low vibrational state densities at reactive energies.[13,58]

The RRKM time constants $(k(E)^{-1})$ for dissociative chemisorption and desorption of the surface PCs for CH_4/Pt(111) are given in Fig. 13. At reactive energies appropriate to thermal and molecular beam dissociative sticking experiments, the time constant for desorption is 2.7 ps which is much shorter than the time constant for dissociation. Consequently, in order for RRKM theory to be applicable to dissociative chemisorption (or desorption) it is the desorption time that must be long compared to the time for microcanonical equilibration of the PCs via IVR. The point is that a microcanonical distribution appropriate for the RRKM rate constant should be established and maintained over the majority of the time available for reaction, in this case only 2.7 ps. Similar requirements have been successfully met for the high pressure RRKM unimolecular decomposition of hydrocarbons where deactivating gas phase collisions (e.g., $\tau_{coll} = 2.7$ ps at 20 bar for $CH_{4(g)}$ at 800 K) set a minimum time scale for IVR as low as 200 fs.[63] In the case of methane dissociative chemisorption, the PCs are prepared collisionally and those formed at a given energy E will have a wide range of different initial phases of vibration, molecular angles toward the surface, and positions across the surface unit cells. Consequently, the initial act of collisional preparation is likely to create an ensemble of PCs that covers a broad range of phase space that may closely resemble a microcanonical ensemble. Indeed, Freed has argued that such collisional preparation alone, without IVR, is sufficient for RRKM kinetics to apply in the mean when averaged over an ensemble of molecules.[64] Here we take the view that collisional preparation of the PCs should produce a quasimicrocanonical ensemble very quickly in the aggregate with very modest requirements for initial state mixing by the reactive potential.[5] Afterwards, attainment and maintenance of

a microcanonical distribution for individual PCs requires IVR time scales to be less than the 2.7 ps desorption time. This rapid IVR requirement seems likely to be met based on analogy to IVR rates of similar gas phase molecules discussed above at both nonreactive and reactive energies. Finally, it should be noted that in the PC–ME implementation of our model we estimated that vibrational energy exchange between the PCs and the surrounding metal is likely to occur every 91 fs (ω^{-1}) which would typically lead to 30 collisions before desorption. Given that the collision step-size distribution is fairly symmetrical in vibrational energy transfer at reactive surface temperatures [Fig. 8(a)], this energy exchange process may also be helpful in establishing and maintaining a microcanonical distribution of PCs on a time scale short compared to desorption. In light of these estimates for rapid microcanonical equilibration of the PCs at reactive energies and the apparent success of the PC–MURT and PC–ME in describing the $CH_4/Pt(111)$ dissociative sticking coefficients, a statistical RRKM treatment of the surface kinetics seems reasonable.

Finally, it is worth pointing out that apart from any time scale arguments, use of the microcanonical sticking coefficient in the PC–MURT for dissociative chemisorption can likely be justified on simple statistical grounds. Recalling Eq. (27) for competitive desorption and dissociation, the dissociative sticking coefficient for a physisorbed complex formed at energy E^* is

$$S(E^*) = \frac{W_R^{\ddagger}(E^* - E_0)}{W_R^{\ddagger}(E^* - E_0) + W_D^{\ddagger}(E^*)}, \qquad (27)$$

which is simply the ratio of the available exit channels through the reactive transition state leading to chemisorbed dissociation fragments to the total number of exit channels available through either the reactive or desorptive transition states. Given that at reactive energies the PC density of states is already huge $[\rho(E^* \geq E_0) > 10^6 \text{ states/cm}^{-1}]$ and the number of available exit channels is vast [e.g., $W_D^{\ddagger}(E^* \geq E_0) > 10^7$ states], the statistical premise that all exit channels at total energy E^* have equal *a priori* probability of being accessed is the simplest assumption that one can make and this returns Eq. (27) above.

E. Sticking from an ambient gas in thermal equilibrium with the surface

Molecular beam dissociative chemisorption[30,51] and thermal associative desorption experiments[46,49] have already been performed for the $CH_{4(g)} \leftrightarrow CH_{3(c)} + H_{(c)}$ reactions on Pt(111). Thermal dissociative sticking coefficients for the methane/Pt(111) system are likely to be measured in the near future. In anticipation of such experiments we have simulated the initial sticking coefficients for CH_4 and CD_4 on Pt(111) under thermal equilibrium conditions and calculated the isotope effect using the PC–MURT parameters derived above from simulation of the molecular beam data. Note that at thermal equilibrium the constraint of detailed balance provides for no net collisional energy transfer between thermalized physisorbed complexes and the surrounding substrate. Accordingly, at thermal equilibrium the PC–ME and PC–

MURT implementations of our model are very similar due to the modest effect of the energy transfer terms in the Master equation, Eq. (22), because the modes of the physisorbed complexes are, for the most part, the same as those of the thermalized gas and surface. In this section and the next we employ the simpler PC–MURT and take $E^* = E - E_{ad}$ as the natural energy scale for which the energy zero is taken to be the molecule at infinite separation from the surface.

Calculation of the initial dissociative sticking coefficient of methane on Pt(111) from a thermally equilibrated ambient gas follows the same general procedure outlined in Sec. IV A for a molecular beam. We first formulate the physisorbed complex energy distribution from the internal and surface energy distributions and the microcanonical sticking coefficient from the sums of states at the transition states. However, averaging of the microcanonical sticking coefficient over the distribution of physisorbed complexes must be taken one step further than for the molecular beam case because molecules from a thermal ambient gas strike the surface from many angles. For this reason, contact with experiment is made through the energy and angle averaged sticking coefficient. Equation (29) must be replaced by

$$S(T) = \int_0^{2\pi} \int_0^{\infty} S(E^*) \, f_T(E^*, \Omega) \, dE^* \, d\Omega, \qquad (62)$$

where $f_T(E^*, \Omega)$ is the incidence angle dependent thermal energy distribution of the physisorbed complex flux and the angular integration is carried out over the forward hemisphere only. Although in principle the microcanonical sticking coefficient may also depend on the incidence direction $d^2\Omega(\vartheta, \varphi)$ of the incoming molecules, we assume it to be angle independent. The thermal sticking coefficient is only indirectly modulated by the direction of the incoming molecules because only the normal translational energy, $E_n = E_t \cos^2(\vartheta)$, is an active translational degree of freedom.

In contrast to the molecular beam case, molecules striking a surface from a thermally equilibrated ambient gas have an equilibrium energy distribution with all degrees of freedom characterized by a single temperature. The rotational and vibrational energy distributions are formulated as in Eqs. (50) and (51) except with $T_r = T_v = T$. The appropriate translational energy distribution for the impinging flux of a thermal ambient gas is the flux-weighted Maxwell–Boltzmann distribution. In spherical polar coordinates the probability distribution for incident molecules to have translational energy from E_t to $E_t + dE_t$ in solid angle $d^2\Omega(\vartheta, \varphi) = \sin(\vartheta)d\vartheta \, d\varphi$ is

$$f_t^*(E_t, \vartheta) = \frac{d^2 f_t(E_t)}{\sin(\vartheta)d\vartheta \, d\varphi} = \frac{\cos(\vartheta)}{\pi} \frac{E_t}{(k_b T)^2} \exp\left(-\frac{E_t}{k_b T}\right), \qquad (63)$$

where ϑ is the polar angle measured from the surface normal. The energy distribution of the local cluster of surface oscillators in the physisorbed complex is given by Eq. (52) with $T_s = T$.

At this point, a particularly simple form for the thermal sticking coefficient may be derived from Eqs. (62), (63), and (44). Because we have assumed the microcanonical sticking

coefficient to be angle independent, the angular integration in Eq. (62) only effects the thermal energy distribution of the physisorbed complexes. Substitution of Eq. (63) into Eq. (44) and integration over the forward hemisphere gives the angle integrated energy distribution of the physisorbed complexes,

$$f_T(E^*) = \int_0^{\pi/2} \int_0^{2\pi} \int_0^{E^*/\cos^2\vartheta} f_i[E^* - E_t\cos^2(\vartheta)]$$

$$\times f_t^*(E_t, \vartheta) \; \sin(\vartheta) \; dE_t \, d\varphi \, d\vartheta, \qquad (64)$$

where as usual only normal translational energy is actively coupled to the physisorbed complex reaction channels. The angular integration in Eq. (64) may be done analytically by changing variables to normal energy, $E_n = E_t \cos^2(\vartheta)$. The result is

$$f_T(E^*) = \frac{1}{k_bT} \int_0^{E^*} f_i[E^* - E_n] \; e^{-E_n/k_bT} \, dE_n, \qquad (65)$$

where E_n is the normal translational energy. Finally, the thermal sticking coefficient is given quite simply as

$$S(T) = \frac{1}{k_bT} \int_0^\infty S(E^*) \int_0^{E^*} f_i(E^* - E_n) \; e^{-E_n/k_bT} \, dE_n \, dE^*. \qquad (66)$$

Figure 14(a) displays the thermal dissociative sticking coefficients for both CH_4 and CD_4 on Pt(111) as a function of temperature calculated from Eq. (66). For each isotope a generalized Arrhenius-type form,

$$S(T) = AT^m \exp\left(-\frac{E_0}{k_bT}\right), \qquad (67)$$

with temperature dependent pre-exponential was found to quite faithfully represent the data until $S(T)$ exceeded $\sim 10^{-2}$ at about 1000 K. Given that the thermal sticking coefficient must eventually roll over with increasing temperature to a limiting value of 1, and $S(E) \approx k_R(E)/k_D(E)$ when $k_R(E) \ll k_D(E)$ (see Fig. 13), it is reasonable that Eq. (67) should apply only to some finite high temperature where $S(T) \ll 1$. By fitting the Eq. (67) form to each set of calculated sticking coefficients an activation energy can be extracted for each isotope as

$$E_a = -k_b \frac{\partial(\ln S(T))}{\partial(1/T)} = E_0 + mk_bT. \qquad (68)$$

The best fits to Eq. (67) over the temperature range $250 \leq T \leq 1000$ K are the curves of Fig. 14(a) where m is 1.76 for CH_4 and 1.89 for CD_4. Predictions for the thermal activation energy of both isotopes at 500 K are given in Fig. 14(a). In addition, Fig. 14(b) shows the ratio of the simulated thermal dissociative sticking coefficients for CH_4 and CD_4 on Pt(111). Clearly, CH_4 dissociatively chemisorbs more readily than CD_4 at all finite temperatures and the limiting value of the kinetic isotope effect is 1 as T tends to infinity.

F. Thermal activation energy

Within the statistical model it is possible to obtain a Tolman expression[65] for the thermal activation energy, E_a,
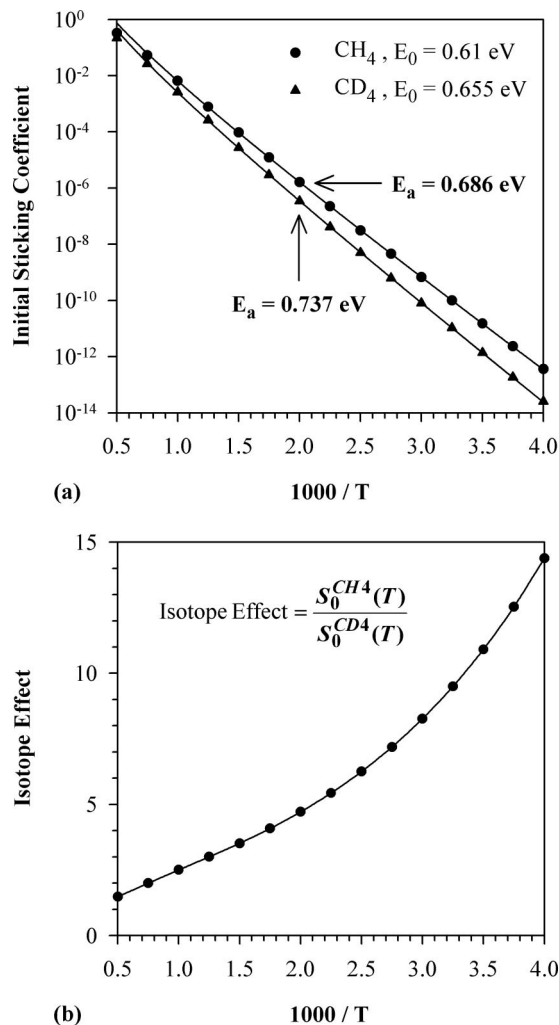

(a) 1000 / T

(b) 1000 / T

FIG. 14. (a) PC–MURT predictions for the thermal dissociative sticking of methane on Pt(111). Activation energies, $E_a = -k_b \; \partial(\ln S)/\partial(1/T)$, derived from best fit to the predictions over the range $1.0 \leq 1000/T \leq 4.0$ yields $E_a = E_0 + mk_bT$ where m is 1.76 for CH_4 and 1.89 for CD_4. (b) PC–MURT prediction of the isotope effect for thermal dissociative sticking of methane on Pt(111).

for dissociative chemisorption of an ambient gas in thermal equilibrium with the surface. The derivation parallels those given by Fowler and Guggenheim[66] for bimolecular and unimolecular reactions ending in the well known result that the activation energy is the difference between the average energy of the reacting complexes and the average energy of all the reactants. In addition, it is also possible to derive a useful approximate result for the thermal activation energy that may rationalize the phenomenological parametrization of Eqs. (67) and (68).

To derive an expression for E_a, we write the thermal sticking coefficient as in Eq. (62),

$$S(T) = \int_0^\infty S(E^*) f_T(E^*;T) dE^*, \qquad (69)$$

where it is assumed that the angular integration over the forward hemisphere has already been performed and the temperature dependence is explicitly included in $f_T(E^*;T)$. To better expose the temperature dependence of $f_T(E^*;T)$, we note that this distribution is formed by convolution of the energy distributions for all active modes of the incident gas and surface and write $f_T(E^*;T)$ as

$$f_T(E^*;T) = \frac{\rho_{gs}(E^*)}{Q_g(T)Q_s(T)} e^{-E^*/k_bT}, \tag{70}$$

where $\rho_{gs}(E^*)$ is the convoluted density of states and $Q_g(T)$ and $Q_s(T)$ are the partition functions of the active degrees of freedom of the incident gas-phase molecules and surface. It is important to note that any active translational modes of the incident molecules are implicitly included in $\rho_{gs}(E^*)$ and $Q_g(T)$ and that all such modes are flux weighted because the reactant gas is only the gas that strikes the surface. Combining Eqs. (69) and (70), the thermal sticking coefficient can be written as

$$S(T) = \frac{1}{Q_g(T)Q_s(T)} \int_0^\infty S(E^*)\rho_{gs}(E^*)e^{-E^*/k_bT} \, dE^*, \tag{71}$$

where all temperature dependent terms are explicitly visible.

Using Eq. (71), the thermal activation energy is easily obtained from its definition [see Eq. (68)] as

$$E_a = k_b T^2 \frac{\partial(\ln S(T))}{\partial T} \tag{72}$$

$$= \frac{\int_0^\infty S(E^*)\rho_{gs}(E^*)E^*e^{-E^*/k_bT}dE^*}{\int_0^\infty S(E^*)\rho_{gs}(E^*)e^{-E^*/k_bT}dE^*}$$

$$- k_b T^2 \frac{\partial(\ln Q_g(T))}{\partial T} - k_b T^2 \frac{\partial(\ln Q_s(T))}{\partial T}. \tag{73}$$

The first term in Eq. (73) simply gives the mean energy of those physisorbed complexes, out of all the physisorbed complexes initially formed, that go on to react $\langle E_{gs}(T)\rangle_R$. The second and third terms in Eq. (73) give the mean energies of the active degrees of freedom of the incident gas phase molecules $\langle E_g(T)\rangle$, and surface $\langle E_s(T)\rangle$, respectively. The thermal activation energy, E_a, can now be written in the particularly simple form,

$$E_a = \langle E_{gs}(T)\rangle_R - (\langle E_g(T)\rangle + \langle E_s(T)\rangle). \tag{74}$$

Equation (74) indicates that the thermal activation energy for dissociative chemisorption is the difference between the average energy of the physisorbed complexes that go on to react and the average energy of all molecules striking the surface and all local clusters of surface oscillators. As usual, E_a is the difference between the average energy of the reacting complexes and the average energy of all the reactants (i.e., all physisorbed complexes formed).

Although a simpler analytic expression for E_a could not be found, it is possible to derive a convenient and fairly accurate approximate expression. Let us begin with Eq. (27) for the microcanonical sticking coefficient,

$$S(E^*) = \frac{k_R(E^*)}{k_R(E^*) + k_D(E^*)}, \tag{75}$$

where $k_R(E^*)$ and $k_D(E^*)$ are the microcanonical rate constants for reaction and desorption. For the methane/Pt(111) systems considered here, this expression can be simplified by noting that at reactive energies ($E^* \geqslant E_0$) the RRKM derived rate constant for desorption is approximately constant (see Fig. 13), $k_D(E^*;E^* \geqslant E_0) \sim \bar{k}_D$. In addition, it is generally true that $k_R(E^*) \ll k_D(E^*)$ in the reactive energy regime (see Fig. 13). Although rigorously this inequality is only valid up to a finite energy $E' \geqslant E_0$, the exponential weighting in the integral of Eq. (71), introduced by $f_T(E^*;T)$, means that the energy region just above the barrier to reaction contributes most significantly to the thermal sticking coefficient. Consequently, for reactive energies appropriate to thermal sticking where $S(T) \lesssim 10^{-2}$, Eq. (75) can now be approximated as

$$S(E^*;E^* \geqslant E_0) \approx \frac{k_R(E^*)}{\bar{k}_D}, \tag{76}$$

where $S(E^*)$ is identically zero for $E^* < E_0$.

Combining Eqs. (71) and (76), the approximate thermal sticking coefficient can be written as

$$S(T) \approx \frac{1}{\bar{k}_D Q_g(T)Q_s(T)} \int_{E_0}^\infty k_R(E^*)\rho_{gs}(E^*)e^{-E^*/k_bT} \, dE^*. \tag{77}$$

Introducing the RRKM form for the microcanonical rate constant for reaction [see Eq. (10)], Eq. (77) becomes

$$S(T) \approx \frac{1}{h \, \bar{k}_D Q_g(T)Q_s(T)} \int_{E_0}^\infty W_R^\ddagger(E^* - E_0)$$

$$\times \frac{\rho_{gs}(E^*)}{\rho(E^*)} e^{-E^*/k_bT} \, dE^*, \tag{78}$$

where $\rho(E^*)$ is the density of states of the physisorbed complex and $W_R^\ddagger(E^* - E_0)$ is the sum of states at the reaction transition state. At this point it is important to note that while $\rho_{gs}(E^*)$ and $\rho(E^*)$ have many modes in common, they are not equal, $\rho_{gs}(E^*) \neq \rho(E^*)$. For example, the rotational modes contained in $\rho_{gs}(E^*)$ are those of the gas phase molecule while in $\rho(E^*)$ these modes have been replaced by the frustrated rotations of the physisorbed molecule. In the interest of making further progress, we replace the density of states ratio in Eq. (78) with its average value over the reactive energy regime,

$$\left\langle \frac{\rho_{gs}(E^*)}{\rho(E^*)} \right\rangle$$

$$= \int_{E_0}^\infty \frac{\rho_{gs}(E^*)}{\rho(E^*)} e^{-E^*/k_bT} \, dE^* \bigg/ \int_{E_0}^\infty e^{-E^*/k_bT} \, dE^* = c. \tag{79}$$

With this approximation, Eq. (78) can be written as

$$S(T) \approx \frac{c}{h\, \bar{k}_D Q_g(T) Q_s(T)} \int_0^\infty W_R^\ddagger(E^* - E_0) e^{-E^*/k_b T} \, dE^*,$$

$$(80)$$

where the integral on the right-hand side can be evaluated using the substitution $E' = E^* - E_0$ followed by integration by parts,

$$\int_0^\infty W_R^\ddagger(E - E_0) e^{-E/k_b T} \, dE = k_b T Q_R^\ddagger(T) e^{-E_0/k_b T}, \quad (81)$$

to give

$$S(T) \approx \frac{c}{\bar{k}_D} \frac{k_b T}{h} \frac{Q_R^\ddagger(T)}{Q_g(T) Q_s(T)} e^{-E_0/k_b T}. \quad (82)$$

Evaluating Eq. (72) with the approximate $S(T)$ of Eq. (82) yields

$$E_a \approx k_b T^2 \left(\frac{1}{T} + \frac{E_0}{k_b T^2} + \frac{\partial(\ln Q_R^\ddagger(T))}{\partial T} - \frac{\partial(\ln Q_g(T))}{\partial T} \right.$$

$$\left. - \frac{\partial(\ln Q_s(T))}{\partial T} \right), \quad (83)$$

where the last three terms simply give the mean energies of the specified degrees of freedom,

$$E_a \approx E_0 + k_b T + \langle E_R^\ddagger(T) \rangle - \langle E_g(T) \rangle - \langle E_s(T) \rangle. \quad (84)$$

Note that $\langle E_g(T) \rangle$ includes the flux-weighted active translational energy of the incident molecules, and $\langle E_R^\ddagger(T) \rangle$ is evaluated with the reaction coordinate degree of freedom removed.

For the dissociative chemisorption of methane on Pt(111), the last three terms of the approximate expression, Eq. (84), for the thermal activation energy are easily evaluated due to cancellation of active modes that are shared by the reaction transition state, the incident gas phase molecules, and the surface. For this system the active modes that do not cancel in Eq. (84) include the four grouped vibrational modes of the physisorbed complexes characterized by the frequency ν_D, one ν_3 antisymmetric C–H stretch vibrational mode identified as the reaction coordinate, the three fully developed rotational modes, and the flux-weighted normal translational mode of the incident methane. Assuming sufficiently high temperatures such that the classical limits are reached for the rotations and translations, our approximate result for E_a becomes

$$E_a \approx E_0 + k_b T + 4\langle E_v(\nu_D, T) \rangle - \langle E_v(\nu_3, T) \rangle - \tfrac{3}{2} k_b T - k_b T, \quad (85)$$

$$E_a \approx E_0 + 4\langle E_v(\nu_D, T) \rangle - \langle E_v(\nu_3, T) \rangle - \tfrac{3}{2} k_b T. \quad (86)$$

Evaluating Eq. (86) at 500 K and recasting the results in the phenomenological form of Eq. (68) gives, $E_a \approx E_0 + 1.9 k_b T$ for CH_4 and, $E_a \approx E_0 + 2.0 k_b T$ for CD_4. These approximate m values are in excellent agreement with those given above in Sec. IV E.

V. DISCUSSION

A. Comparison to experiment

Let us now return to more critically examine any discrepancies between our theoretical modeling and predictions and the results of experiments. Using all the experimental data of Fig. 3, a single set of the three free parameters of the PC–MURT was chosen by minimizing the average relative discrepancy between theoretical simulations and the experimental results. Final agreement between theory and experiment is excellent for the 680 K nozzle temperature data at translational energies greater than 0.4 eV for both CH_4 and CD_4. At energies $E_t < 0.4$ eV, the theory increasingly tends to overestimate the sticking as the translational energy is reduced. This effect is believed to be due to increasing vibrational cooling of the molecular beam as the gas seeding mixture of methane is increased to obtain slower beams while the theoretical simulations always maintain that the methane vibrational temperature, T_v, is equal to the nozzle temperature T_n. If vibrational cooling is experimentally occurring in the beam so that $T_v < T_n$, then the simulations are assuming that there is more vibrational energy in the incident methane molecules than there really is and, of course, the sticking is correspondingly overestimated.

The IBM supersonic molecular beam experiments were performed by seeding various mole percentages of methane in H_2, He, and Ar at fixed nozzle temperatures.[30,51] For a beam of a pure ideal gas whose gas temperature has been thermalized to that of the nozzle before its supersonic expansion (i.e., $T_g = T_n$), the final translational energy of the beam is determined by the nozzle temperature as $E_t = \tfrac{5}{2} k_b T_n$. Consequently, to vary the methane translational energy at fixed T_n it is necessary to introduce or "seed" methane at various percentages into beams of other "carrier" gases whose velocities at the final $\sim \tfrac{5}{2} k_b T$ energy of the beam may be higher or lower than methane depending on their mass. The disparate velocities of methane and the other gases in the beam leads to collisional buffeting of the methane during the supersonic expansion and a controlled manipulation of the methane E_t becomes possible by varying the gas mixture of the beam. Although the IBM authors do not report on the details of their seeding mixtures versus methane E_t, using the beam calculations of Chorkendorff and co-workers[8] the range of CH_4 translational energies accessible at $T_n = 680$ K using binary gas mixtures is 1.17 eV $\geqslant E_t \geqslant 0.23$ eV for 1% to 100% CH_4 in H_2, 0.57 eV $\geqslant E_t \geqslant 0.23$ eV for 1% to 100% CH_4 in He, and 0.23 eV $\geqslant E_t \geqslant 0.059$ eV for 100% to 1% CH_4 in Ar. The methane energy range accessible using binary mixing with Ar was not employed in the IBM experiments but Ar might have been used as a secondary diluent to H_2 or He in tertiary gas mixtures. Importantly, the calculations above suggest, and we will assume, that the CH_4 E_t scan at $T_n = 680$ K of Fig. 3 from $E_t = 1.17$ eV to 0.23 eV was accomplished with gas seeding mixtures varying from 1% CH_4 in H_2 at the highest energy through to 100% CH_4 at the lowest energy.

Unfortunately, vibrational cooling of molecules in supersonic molecular beams (i.e., $T_v < T_n$) is difficult to measure and a quantitative theory of the nonequilibrium process is

lacking. Vibrational hot-band analysis[67–69] of rovibrational or electronic spectra of beam molecules provides the most definitive determination of T_v. For larger polyatomic molecules, photoionization threshold spectroscopy[70] and fragmentation following electron impact ionization[71] can also be used to estimate T_v. It is generally found that vibrational cooling increases as the beam carrier gas is varied from monatomic $<$ diatomic $<$ polyatomic molecules. Amongst the monatomic gases, Ar, Kr, and Xe have proven to be particularly efficient at cooling some large polyatomic molecules to $T_v < 50$ K.[69] A potentially troublesome issue is that vibrational cooling need not be uniform across the different vibrational modes of a molecule.[72] For example, the ν_1 and ν_2 vibrations of SO_2 were cooled in a seeded He beam expansion from room temperature to 235 and 140 K, respectively.[68] In contrast, although I_2 can be cooled to $T_v \sim 50$ K,[67] the relatively high frequency vibrations of most diatomic molecules leads to very inefficient vibrational cooling because of the large mismatch between their vibrational and translational or rotational energy quanta. For polyatomic molecules, two vibrational quanta + translational energy exchange processes are likely to be efficient agents of vibrational cooling because if one vibrational mode is de-excited while another is excited it is only the difference in the vibrational energies that must be removed as translation.[70] In bimolecular collisions between polyatomic molecules such $v_- v_+ t$ exchanges should be more probable as will be opportunities for longer lived complexations leading to more statistical energy exchange. For CH_4, the energy difference between vibrational modes can be quite small, $\nu_3 - \nu_1 = 106$ cm^{-1} and $\nu_2 - \nu_4 = 220$ cm^{-1}, smaller or comparable to the vibrations of I_2. Consequently, although the relatively high frequency individual vibrations of methane may not cool appreciably when expanded at low concentration in H_2 or He carrier gases (like most diatomics) there is reason to believe that vibrational cooling will increase as the methane concentration increases and more intermethane collisions occur.

To date, in the absence of spectroscopic studies, it has invariably been assumed that $T_v = T_n$ for methane in molecular beam dissociative chemisorption studies. The excellent agreement between theory and experiment in Fig. 3 for CH_4 dissociative sticking over the range 1.17 eV $\geq E_t > 0.4$ eV at $T_n = 680$ K, where CH_4 was seeded from 1% CH_4 in H_2 to as little as 20% CH_4 in He, suggests that $T_v = T_n$ is a reasonable assumption here. Similarly, the CD_4 sticking predictions over the 1.3 eV $\geq E_t \geq 0.83$ eV range, where the H_2 seeded beam was less than 11% CD_4, are excellent and consistent with $T_v = T_n$. However as noted above, theory increasingly overestimates the CH_4 sticking as E_t falls over the range from 0.4 eV $\geq E_t \geq 0.23$ eV at $T_n = 680$ K and the % CH_4 seeding in the beam increases from 20% to 100%. We suspect this increasing discrepancy between theory and experiment is due to increasing vibrational cooling in the molecular beam as the CH_4 concentration of the beam climbs above $\sim 20\%$.

Interestingly the theoretical predictions of the CH_4 sticking data at $T_n = 300$ K displayed in Fig. 3 consistently underestimate the experimental sticking. One complication is
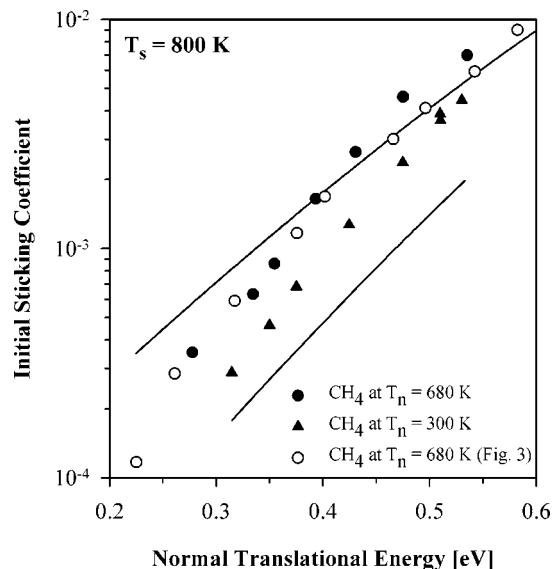

FIG. 15. Comparison of PC–MURT simulations for CH_4 dissociative sticking on Pt(111) as a function of normal translational energy at two nozzle temperatures with data from molecular beam experiments (Ref. 30).

that these $T_n = 300$ K experimental sticking points derive from a separate experimental study by Bethune and Luntz[30] that was specifically designed to investigate the effect of changing vibrational energy on sticking and employed a different data analysis that accounted for the varying widths of the beam translational energy distributions as E_t was varied. The data of this second experimental study at $T_n = 680$ and 300 K, along with our theoretical predictions are reproduced as the black points and lines in Fig. 15. The open experimental points at $T_n = 680$ K are comparable data taken from the separate Fig. 3 experimental run and provide some sense of the experimental reproducibility and the effect of altered data analysis. Importantly, the consistently derived filled experimental sticking data of Fig. 15 indicate that sticking is increased by a factor of ~ 2 as T_n is increased from 300 to 680 K over the range of translational energies where we calculate the CH_4 seeding ranged from 4% to 60% in He at $T_n = 680$ K and from 1% to 14% in H_2 at $T_n = 300$ K. Our theoretical predictions indicate the sticking should have increased by a factor of ~ 3 as T_n was increased from 300 to 680 K.

An interesting question is whether the vibrational temperature of the methane gas in heated nozzles actually equilibrates to the nozzle temperature before its expansion. This is not a problem for a room temperature beam because all the plumbing leading up to the nozzle is already at room temperature. For heated nozzles, the question reduces to whether the number of collisions the molecules experience as they traverse the heated portion of the nozzle is sufficient for internal energy equilibration to the final nozzle temperature. In laboratory studies of nozzle design, Mullins has found that for simple straight nozzles, for some combinations of stagnation pressure and nozzle diameter, even translational equilibration of pure He gas can lag the nominal nozzle temperature unless the nozzle is heated over at least 9 inches of its length (e.g., heating the last 2 inches of a straight nozzle

to 900 K brought the He gas temperature up to only 600 K).[73] Presumably, internal energy equilibration of polyatomic molecules to the nozzle temperature is more difficult than translational equilibration because of relatively inefficient collisional energy exchange coupling to vibrations.

The Fig. 5 predictions of sticking versus $1/T_n$ (assuming $T_n = T_v$) over the 0.3–0.5 eV beam translational energy range suggest that the Fig. 15 data at $T_n = 680$ K would be modulated ~2-fold if the methane T_v systematically lagged T_n by 100 K, either through incomplete internal equilibration of the gas in the nozzle prior to supersonic expansion or by vibrational cooling during expansion. Clearly, the Fig. 15 $T_n = 680$ K data are predicted to be quite sensitive to any lag of T_v from T_n and are complicated by a % CH_4 seeding range that crosses the ~20% level where vibrational cooling is believed to become significant. Nevertheless, the Fig. 15 agreement between theoretical predictions (assuming $T_v = T_n$) and experiments remains relatively poor, particularly for the $T_n = 300$ K data. If we assume for a moment that the entire experimental data set of Fig. 3 at $T_n = 680$ K suffered from a known amount of vibrational temperature lag or cooling, then it might well be possible to re-simulate the data to find optimal new PC–MURT parameters that would simultaneously agree with the Figs. 3 and 15 experiments. For example, according to Fig. 5, if T_v lagged T_n by ~100 K at $T_n = 680$ K, then the Fig. 15 experimental ratio of ~2 for sticking at $T_n = 680$ K versus 300 K could be reproduced. Unfortunately, T_v has never been characterized in methane molecular beam experiments. We choose not to re-simulate the data using T_v as a new free parameter of our model. Instead let us restate that the current optimization of the three PC–MURT parameters under the assumption that $T_v = T_n$ should yield an upper bound for E_0 if the true experimental data suffers some lag or cooling of T_v from T_n. The theory will then overestimate the vibrational energy in the molecules and must posit a higher barrier to return the measured experimental sticking coefficient. *Complementary to the earlier discussion in Sec. IV C, it appears that optimizing the PC–MURT parameters by simulation of experimental data under the assumption that $T_v = T_n$ will yield an upper bound for E_0.*

The Fig. 4 experimental data derive from two different molecular beam machines and the agreement with the PC–MURT theoretical predictions is really quite good. Broadly consistent with the vibrational cooling discussion above, the worst agreement is at the lowest E_t where the CH_4 seeding is calculated to be the highest, at 18%.

The thermal dissociative sticking predictions for methane on Pt(111) are displayed in Fig. 14. The activation energy for CH_4 chemisorption at 500 K is predicted to be $E_a = 0.686$ eV. Although experimental studies of the thermal sticking of methane on Pt(111) are lacking, Sun and Weinberg[74] have measured an effective activation energy, $E_a(T_s)$, of 0.624 eV for 300 K CH_4 gas incident on a Pt(110)−(1×2) surface by varying the surface temperature. The more open Pt(110) surface is generally more reactive than the close-packed Pt(111) surface and it is expected that the equilibrium activation energy for methane chemisorption on Pt(110) should be lower. However, because the Weinberg

experiments were done at fixed gas temperature, $T_g = 300$ K, and variable surface temperature 1000 K$\geqslant T_s \geqslant 400$ K, rather than with $T_g = T_s$ as in the CH_4/Pt(111) equilibrium simulations of Fig. 14, the resulting effective activation energy and sticking coefficients are nonequilibrium ones. Such nonequilibrium sticking is easily handled within the PC–MURT model and will be discussed further below. Here, let us simply note that the relatively depressed $T_g = 300$ K of the CH_4/Pt(110) chemisorption experiments leads to about an order of magnitude less sticking than the Fig. 14 predictions for CH_4/Pt(111) where $T_g = T_s$.

B. Comparison to theory

The PC–MURT parameters for CH_4 dissociative chemisorption on Pt(111) derived by optimizing simulations to all the dissociative sticking data of Fig. 3 under the premise that $T_v = T_n$ are the apparent reaction threshold energy, $E_0 = 0.61$ eV (over a C–H stretch reaction coordinate); a lumped low frequency representative of the $CH_4 -$ Pt stretching mode along the surface normal and the frustrated rotations within the physisorption potential well, $\nu_D = 110$ cm^{-1}; and the number of surface vibrational modes that can freely exchange energy in the local adsorbate–surface complex, $s = 3$. These values compare favorably to the $E_0 = 0.635$ eV, $\nu_D = 130$ cm^{-1}, and $s = 3$ values obtained by Ukraintsev and Harrison[5] in an earlier implementation of a PC–MURT that contained many approximations to facilitate numeric calculations. The predictions of an alternative thermally assisted tunneling model[51] for dissociative chemisorption of CH_4 on Pt(111) are almost uniformly in discrepancy with experiment by 1 to 2 orders of magnitude and predict a three fold greater kinetic isotope effect than is experimentally observed. Given the excellent agreement of the PC–MURT with experiment, including the kinetic isotope effect, we believe that tunneling is insignificant in methane dissociative chemisorption and that dissociation occurs primarily via an ordinary "over the barrier" mechanism.

Electronic structure theory (EST) calculations for CH_4 dissociation on Pt(111) have provided a variety of estimates for the apparent reaction threshold energy, E_0. Using a 10-atom cluster model of Pt(111) and the atom superposition and electron delocalization molecular orbital (ASED–MO) method, Anderson and Maloney calculated $E_0 = 0.45$ eV.[75] The semiempirical bond-order conservation Morse-potential (BOC–MP) method has been used to estimate $E_0 = 0.84$ eV[76] and $E_0 = 0.78$ eV.[77] More recently, generalized gradient approximation density functional theory (GGA–DFT) calculations yield $E_0 = 0.66$ eV.[78] The most sophisticated *ab initio* EST calculations for methane dissociative chemisorption were made by Yang and Whitten for CH_4 on Ni(111), not Pt(111), where they found $E_0[CH_4/Ni(111)] = 0.72$ eV.[10] The Whitten calculations indicate that although the transition state for methane dissociation on the Ni(111) surface is primarily over an atop site the dissociation products must ultimately separate to occupy nearby sites with higher coordination. We assume that similar dissociation energetics apply for CH_4/Pt(111),[79] a system that is experimentally found to be more active than CH_4/Ni(111) and consequently

presumed to have a lower E_0. The $E_0[\text{CH}_4/\text{Pt}(111)]$ $=0.61$ eV determined in this paper by PC–MURT analysis of the IBM molecular beam data appears to represent a reasonable upper bound for the true reaction threshold energy.

The number of surface oscillators participating in free exchange of energy within the $\text{CH}_4/\text{Pt}(111)$ physisorbed complex was determined to be $s=3$. Given that the dissociative sticking coefficient obeys normal energy scaling and the molecular translational energy parallel to the surface was treated as inactive and as a conserved quantity, the surface oscillators are logically constrained to be incapable of exchanging parallel translational energy. Therefore, the PC–MURT model suggests that three surface oscillators acting in the direction of the surface normal participate in energy exchange within the physisorbed complex and these oscillators presumably derive from three separate and adjacent surface atoms. Interestingly, in poisoning studies of steam reforming on Ni surfaces, the minimum ensemble size of surface atoms required for reaction (rate limited by CH_4 dissociative adsorption) was estimated using a mean field analysis as 2.7,[17] a number quite similar to our estimate of $s=3$ above. More likely relevant is a recent DFT investigation of dissociative chemisorption of CH_4 on Ir(111) that found the surface substantially relaxes at the transition state, with the one Ir atom most directly underneath the reacting CH_4 displaced outwards along the surface normal by 0.41 Å.[80] With this kind of transition state (not generally explored in the past) the surface temperature should strongly influence dissociative chemisorption and several surface atoms would likely be required to participate in the surface relaxation.

C. Reaction dynamics on a multidimensional potential energy surface

One of the primary advantages in using supersonic molecular beam methods to study the dissociative chemisorption of molecules on surfaces is the ability to independently control the translational and internal energy distributions of the incident molecules and the surface thermal distribution. By selective variation of the translational and internal energies of the incident molecules and the surface temperature, it is possible to initially access different regions of the multidimensional potential energy surface governing dissociative chemisorption. Although the multidimensional dissociative sticking data derived from molecular beam experiments can usually be summarized using empirical fitting forms, no rigorous connection has been made between the resulting experimental fit parameters and unique features of the reaction dynamics or the potential energy surface, such as the reaction threshold energy.[12] As shown in Sec. IV, we have derived both exact and approximate expressions within the PC–MURT for the thermal activation energy which provide a connection between the reaction threshold energy and the measured activation energy in thermal experiments. Here we extend our analysis to characterize multidimensional dissociative sticking by deriving theoretical expressions for effective activation energies, efficacy of sticking, and fractional energy uptake parameters that might be experimentally measurable and verifiable.

1. Effective activation energies

As shown in Figs. 4 and 5, the surface and nozzle temperature dependence of the initial dissociative sticking coefficient of methane on Pt(111) is distinctly non-Arrhenius. The slopes of these curves vary markedly with surface temperature, nozzle temperature, and beam translational energy and have no clear relationship to the thermal activation energy, E_a, or the apparent reaction threshold energy, E_0. Within the framework of the PC–MURT it is possible to calculate ''effective activation energies'' from the surface and nozzle temperature dependence of the dissociative sticking coefficient. Another effective activation energy can be derived for the case where a thermal ambient gas at variable temperature T_g is made incident upon a surface at fixed surface temperature. The slopes of these sticking curves and associated effective activation energies are theoretically found to depend on the specific experimental conditions and thus provide no special information about the reactive potential energy surface or dynamics. Of course, the PC–MURT is a statistical microcanonical theory that treats all forms of active energy available to the physisorbed complexes on an equal footing and the total information content of the theory derives from its free parameters (i.e., E_0, ν_D, and s) that can be fixed by simulation of varied experimental data or derived quantities such as effective activation energies. On the other hand, if a dynamical theoretical description of methane dissociative chemisorption is required and the statistical PC–MURT model is inappropriate, there may indeed be more detailed information that can be learned from effective activation energies.

We define the effective activation energy associated with the surface temperature dependence of the sticking coefficient as

$$E_a(T_s) \equiv k_b T_s^2 \frac{\partial (\ln S(T_s))}{\partial T_s}, \qquad (87)$$

where $S(T_s)$ is the surface temperature dependent dissociative sticking coefficient. Following the same approach as our derivation of the thermal activation energy, we expose the surface temperature dependence of the sticking coefficient by writing

$$S(T_s) = \int_0^\infty S(E^*) f(E^*; T_s) dE^*, \qquad (88)$$

where $f(E^*; T_s)$ is the surface temperature dependent initial energy distribution of physisorbed complexes and is given by

$$f(E^*; T_s) = \int_0^{E^*} f_g(E^* - E_s) f_s(E_s; T_s) dE_s. \qquad (89)$$

In Eq. (89), $f_s(E_s; T_s)$ is the energy distribution of the local cluster of surface atoms at temperature T_s and $f_g(E_g)$ is the convoluted energy distribution for all active degrees of freedom of the incident gas phase molecules,

$$f_s(E_s; T_s) = \frac{\rho_s(E_s)}{Q_s(T_s)} e^{-E_s/k_b T_s}. \qquad (90)$$

Combining Eqs. (88)–(90) gives the surface temperature dependent sticking coefficient,

J. Chem. Phys., Vol. 118, No. 2, 8 January 2003

Microcanonical unimolecular rate theory   867

$$S(T_s) = \frac{1}{Q_s(T_s)} \int_0^\infty S(E^*) \int_0^{E^*} f_g(E^* - E_s)$$
$$\times \rho_s(E_s) e^{-E_s/k_b T_s} \, dE_s \, dE^*, \tag{91}$$

and taking the derivative according to Eq. (87) gives

$$E_a(T_s) = \langle E_s(T_s) \rangle_R - \langle E_s(T_s) \rangle, \tag{92}$$

for the effective surface temperature activation energy. In this expression, $\langle E_s(T_s) \rangle_R$ is the mean surface energy of those physisorbed complexes undergoing reaction and $\langle E_s(T_s) \rangle$ is the mean surface energy of all physisorbed complexes formed under the specific experimental conditions.

The nozzle temperature dependence of the sticking coefficient can also be characterized by an effective activation energy,

$$E_a(T_n) \equiv k_b T_n^2 \frac{\partial(\ln S(T_n))}{\partial T_n}. \tag{93}$$

As opposed to $E_a(T_s)$, which specifically relates to the surface degrees of freedom, $E_a(T_n)$ relates to both the vibrational and rotational degrees of freedom of the incident molecules because both are dependent upon the nozzle temperature. To complicate matters further, due to vibrational and rotational cooling of molecules in a supersonic molecular beam expansion, the temperatures T_v and T_r characterizing the energy distributions of these degrees of freedom are certainly less than the nozzle temperature and the exact dependence is currently unknown. Here we simply characterize these temperatures in an empirical way as some fraction of the nozzle temperature such that the vibrational temperature is given as $T_v = \gamma T_n$ and the rotational temperature is given as $T_r = \lambda T_n$. Typical estimates of γ and λ are 1 and 0.1, respectively. As before, we assume canonical energy distributions for the vibrational and rotational degrees of freedom of the molecules in the molecular beam [see Eqs. (50) and (51)],

$$f_j(E_j; T_j) = \frac{\rho_j(E_j)}{Q_j(T_j)} e^{-E_j/k_b T_j}, \tag{94}$$

where j can be either v or r for vibration and rotational distributons, respectively. The nozzle temperature dependent initial energy distribution of physisorbed complexes is then,

$$f(E^*; T_n) = \int_0^{E^*} f_{\text{oth}}(E_{\text{oth}}) \int_0^{E^* - E_i} f_v(E_v; T_v)$$
$$\times f_r(E^* - E_{\text{oth}} - E_v; T_r) dE_v \, dE_{\text{oth}}, \tag{95}$$

where $f_{\text{oth}}(E_{\text{oth}})$ is the convoluted initial energy distribution of all other active modes in the physisorbed complex. The effective activation energy $E_a(T_n)$ can now be obtained by using this expression for $f(E^*; T_n)$ in Eq. (29) for the PC–MURT sticking coefficient and differentiating with respect to T_n according to Eq. (93), being careful to include the nozzle temperature dependence of the rotational and vibrational temperatures. The result is

$$E_a(T_n) = \frac{1}{\gamma} \{ \langle E_v(\gamma T_n) \rangle_R - \langle E_v(\gamma T_n) \rangle \}$$
$$+ \frac{1}{\lambda} \{ \langle E_r(\lambda T_n) \rangle_R - \langle E_r(\lambda T_n) \rangle \}$$
$$= \frac{1}{\gamma} E_a(T_v = \gamma T_n) + \frac{1}{\lambda} E_a(T_r = \lambda T_n), \tag{96}$$

where $\langle E_v(\gamma T_n) \rangle_R$ and $\langle E_r(\lambda T_n) \rangle_R$ are the mean vibrational and rotational derived energies of those physisorbed complexes undergoing reaction and $\langle E_v(\gamma T_n) \rangle$ and $\langle E_r(\lambda T_n) \rangle$ are the mean vibrational and rotational derived energies of all the physisorbed complexes under the specific experimental conditions. In the usual way, effective activation energies associated with the independent variation of the vibrational and rotational temperatures are defined by $E_a(T_v)$ and $E_a(T_r)$. Clearly, the dissociative sticking coefficient has a complex dependence on the nozzle temperature of the molecular beam. To the extent that the incident beam molecules are always well cooled in the rotational degrees of freedom such that the rotational temperature is much smaller than the temperature of the other degrees of freedom [i.e., $f_r(E)$ is narrow and much more sharply peaked near $E=0$ than the other distributions], the rotational contribution to $E_a(T_n)$ in Eq. (96) is relatively small (ca. 3% for $\lambda = 0.1$ and 1), so that,

$$E_a(T_n) \simeq \frac{1}{\gamma} \{ \langle E_v(\gamma T_n) \rangle_R - \langle E_v(\gamma T_n) \rangle \}$$
$$= \frac{1}{\gamma} E_a(T_v = \gamma T_n), \tag{97}$$

can be an excellent approximation.

In the case where a thermal ambient gas at variable temperature T_g is incident upon a surface at temperature T_s we define the gas temperature dependent effective activation energy as

$$E_a(T_g) \equiv k_b T_g^2 \frac{\partial(\ln S(T_g))}{\partial T_g}. \tag{98}$$

With the thermal energy distribution of the active degrees of freedom of the incident gas denoted as $f_g(E_g; T_g)$, the initial energy distribution of physisorbed complexes is

$$f(E^*; T_g) = \int_0^{E^*} f_s(E^* - E_g) f_g(E_g; T_g) dE_g, \tag{99}$$

and the associated effective activation energy is

$$E_a(T_g) = \langle E_g(T_g) \rangle_R - \langle E_g(T_g) \rangle, \tag{100}$$

where the derivation has been carried out in the usual way. In Eq. (100), $\langle E_g(T_g) \rangle_R$ is the mean energy derived from the gas of those physisorbed complexes undergoing reaction and $\langle E_g(T_g) \rangle$ is the mean energy derived from the gas of all the physisorbed complexes under the specific experimental conditions.

2. Efficacy of sticking

The energy dependence of the initial dissociative sticking coefficient measured in supersonic molecular beam experiments is frequently characterized by defining "efficacy of sticking" parameters. These efficacy parameters are usually defined as the logarithmic derivative of the sticking coefficient with respect to the first moment of the distribution of a specific type of energy.[81,82] For example, using a molecular beam it is possible to control both the mean translational energy and the mean vibrational energy of the incident molecules so that one might define a "translational efficacy" as $\beta_t = \partial(\ln S)/\partial\langle E_t\rangle$, and a "vibrational efficacy" as $\beta_v = \partial(\ln S)/\partial\langle E_v\rangle$. It should be noted that the experimental distributions $f_t(E_t)$ and $f_v(E_v)$ are not delta functions and higher moments (e.g. widths) of these distributions (see Fig. 2) are also likely to be important in determining experimentally realized sticking coefficients that theoretically involve convolving the $f_j(E_j)$ distributions and integrating over the microcanonical sticking coefficient (see Figs. 2 and 13). Nevertheless, various authors have used β_t and β_v as a basis for investigating whether a dynamical or statistical model is more appropriate for describing methane dissociative chemisorption. Here we derive expressions for β_t and β_v within the framework of the PC–MURT.

To derive an expression for the translational efficacy parameter, we first formulate the initial energy distribution of the physisorbed complexes with the dependence on the mean translational energy explicitly shown,

$$f(E^*;\langle E_t\rangle) = \int_0^{E^*} f_{\text{oth}}(E^* - E_t)f_t(E_t;\langle E_t\rangle)dE_t. \quad (101)$$

In this expression, $f_t(E^*;\langle E_t\rangle)$ is the translational energy distribution of the molecules in the molecular beam and $f_{\text{oth}}(E_{\text{oth}})$ represents the convoluted initial energy distribution for all other active degrees of freedom of the incident molecules and surface. The initial dissociative sticking coefficient as a function of the mean beam translational energy is then given by

$$S(\langle E_t\rangle) = \int_0^\infty S(E^*) \int_0^{E^*} f_{\text{oth}}(E^* - E_t)f_t(E_t;\langle E_t\rangle)dE_t \, dE^*. \quad (102)$$

Differentiation of the natural logarithm of Eq. (102) with respect to $\langle E_t\rangle$ gives

$$\beta_t = \frac{1}{S} \int_0^\infty S(E^*) \int_0^{E^*} f_{\text{oth}}(E^* - E_t) \frac{\partial f_t(E_t;\langle E_t\rangle)}{\partial\langle E_t\rangle}dE_t \, dE^*. \quad (103)$$

Note that the $\langle E_t\rangle$ dependence of the sticking coefficient arises solely from the translational energy distribution. Further evaluation of Eq. (103) requires specification of a functional form for $f_t(E^*;\langle E_t\rangle)$.

A convenient form for the normalized flux-weighted translational energy distribution of molecules incident on the surface from a supersonic molecular beam is given by Eq. (45). Although an analytic expression for the mean translational energy that would result from averaging E_t over the Eq. (45) distribution can be written down, it is too cumbersome to incorporate explicitly into the distribution function. To circumvent this problem, we note as before that although E_b is not exactly equal to the mean translational energy, they are approximately the same ($\langle E_t\rangle \approx E_b$) for reasonable choices of T_t and E_b. For this reason, we simply replace $\langle E_t\rangle$ with E_b in Eqs. (101)–(103) above to obtain an approximate expression for β_t. Taking the derivative of Eq. (45) with respect to E_b, being careful to include the dependence of the normalization constant on E_b, gives

$$\frac{\partial f_t(E_t;E_b)}{\partial E_b} = \left\{\frac{1}{N}\frac{\partial N}{\partial E_b} + \frac{1}{k_b T_t}\left(\sqrt{\frac{E_t}{E_b}} - 1\right)\right\}f_t(E_t;E_b). \quad (104)$$

Substitution of this derivative into Eq. (103) gives

$$\beta_t \simeq \frac{1}{N}\frac{\partial N}{\partial E_b} + \frac{1}{k_b T_t}\left(\frac{\langle\sqrt{E_t}\rangle_R}{\sqrt{E_b}} - 1\right), \quad (105)$$

for the translational efficacy where $\langle\sqrt{E_t}\rangle_R$ is the mean of the square root of the translation derived energy of those physisorbed complexes undergoing reaction under the specific experimental conditions.

As opposed to our expression for the translational efficacy, a rather simple form for the vibrational efficacy, β_v, can be derived within the framework of the PC–MURT. Noting that

$$\frac{\partial}{\partial\langle E_v\rangle} = \frac{\partial T_v}{\partial\langle E_v\rangle}\frac{\partial}{\partial T_v}, \quad (106)$$

where T_v is the vibrational temperature of the incident molecules and $C_V^v(T_v) = \partial\langle E_v\rangle/\partial T_v$ is their constant volume vibrational heat capacity,

$$\beta_v = \frac{1}{C_V^v(T_v)}\frac{\partial(\ln S)}{\partial T_v} = \frac{E_a(T_v)}{k_b T_v^2 C_V^v(T_v)}. \quad (107)$$

Assuming that the vibrational temperature in this expression is related to the nozzle temperature of the incident molecular beam via $T_v = \gamma T_n$, where γ is a constant, the vibrational efficacy is related to the nozzle temperature dependent effective activation energy derived above, Eq. (97),

$$\beta_v \simeq \frac{E_a(T_n)}{k_b T_n^2 \gamma C_V^v(\gamma T_n)}, \quad (108)$$

as long as the rotational contribution to $E_a(T_n)$ can be safely neglected. This defines a relationship between experimentally derivable quantities that constitutes a prediction of the statistical model. Unfortunately, direct measurement of γ requires vibrational hot band spectroscopy of the molecular beam making evaluation of Eq. (108) difficult.

Luntz and Bethune[30] have pointed out that the sticking of their CH_4 molecular beam on Pt(111) data of Fig. 3 above at $T_s = 800$ K and $T_n = 680$ K is well described by $S = 0.073 \, E_n^{4.27}$ which leads to variable β_t. As E_n increases from 0.2 to 1.3 eV, β_t decreases from $\simeq 20$ to 3 eV^{-1}. By way of comparison, Luntz and Bethune evaluated β_v from their CH_4 beam data of Fig. 15 in which T_n was varied from 680 to 300 K. Assuming $T_v = T_n$ and no contribution to the

TABLE II. Dissociative chemisorption at thermal equilibrium at a temperature of 500 K: Fractional energy uptakes, f_j; mean energy derived from the jth degrees of freedom for complexes undergoing reaction $\langle E_j(T)\rangle_R$; mean energy derived from the jth degrees of freedom for all complexes formed at a temperature T^* $\langle E_j(T^*)\rangle$.

Mode j	f_j	$\langle E_j(T)\rangle_R$ [eV] at $T=500$ K	$\langle E_j(T^*)\rangle$ at $T^*=1350$ K	
		$\langle E^*(T)\rangle_R=0.92$ eV	[eV]	$k_b T^*$
Translation t	0.13	0.12	0.12	1.0
Rotation r	0.18	0.17	0.17	1.5
Vibration ν	0.33	0.30	0.32	2.7
Surface s	0.36	0.33	0.33	2.8

sticking from rotational energy of the incident molecules, they found $\beta_v=12.3$ eV^{-1}. Over the 0.3 to 0.5 eV range of normal translational energy where β_v was evaluated to be constant at 12.3 eV^{-1}, β_t ranged from 14.2 to 8.54 eV^{-1}. Based on these experimental observations and the theoretical analysis given here, it seems likely that β_t and β_v are largely functions of the experimental particulars. Consequently, experimental findings of $\beta_t \neq \beta_v$ may be quite consistent with a statistical theory of dissociative chemisorption and conversely a finding of $\beta_t=\beta_v$ under some experimental conditions is not necessarily supportive.

3. Fractional energy uptake

In order to characterize energy consumption in the dissociative chemisorption of methane on Pt(111), we define fractional energy uptake parameters, f_j, as

$$f_j=\langle E_j\rangle_R/\langle E^*\rangle_R, \tag{109}$$

where $\langle E_j\rangle_R$ is the mean energy derived from the jth degrees of freedom of the molecules or surface that form those physisorbed complexes undergoing reaction and $\langle E^*\rangle_R$ is the mean total energy of those physisorbed complexes undergoing reaction under specific experimental conditions. For the thermal CH$_4$/Pt(111) system at equilibrium at 500 K, Table II gives the fractional energy uptakes from the rotational, vibrational, translational, and surface degrees of freedom, as well as the associated energies for those physisorbed complexes undergoing reaction. Clearly, for the equilibrium system at 500 K, the surface and vibrational degrees of freedom contribute the most energy to the reacting physisorbed complexes and are thus most important in promoting dissociative chemisorption. In the statistical PC–MURT model it is the relative *availability* of different types of energy to form physisorbed complexes with sufficient pooled energy to react

under given experimental conditions that is the key issue in dictating the fractional energy uptakes. Certainly in this microcanonical theory, energy in any active degree of freedom is equally effective in helping to surmount the reaction barrier to dissociative chemisorption so only the relative availability of the different types of energy can matter.

For the thermal CH$_4$/Pt(111) system at 500 K the active degrees of freedom for those physisorbed complexes undergoing reaction can be described by an effective temperature, $T^* \approx 1350$ K. The assignment of an effective temperature to the active degrees of freedom is based on the fact that at the high temperatures potentially descriptive of the reacting complexes, the translational and rotational degrees of freedom of the incident molecules will be in the equipartition limit such that the correspondences $\langle E_t(T)\rangle_R \simeq k_b T^*$ and $\langle E_r(T)\rangle_R \simeq \frac{3}{2}k_b T^*$ can be made. Table II provides a comparison of the calculated $\langle E_j(T^*)\rangle$ to $\langle E_j(T)\rangle_R$ in eV and $k_b T^*$. Note that for a Planck oscillator of frequency ν_0, an oscillator whose energy is measured from its zero point level, the equipartition limit is reached at $\langle E\rangle_{\text{high } T}=k_b T - \frac{1}{2}h \nu_0$. Consequently, the Table II entry for $\langle E_s(T^*)\rangle = 2.8 k_b T^*$ correctly represents the equipartition limit for three surface oscillators at the mean Pt phonon frequency of 122 cm^{-1}. The detailed balance implications of Table II for the reverse reaction, CH$_{3(c)}$ + H$_{(c)} \rightarrow$ CH$_{4(g)}$, in thermal equilibrium under idealized experimental conditions where no additional side reactions are possible [e.g., CH$_{3(c)} \rightarrow$ CH$_{2(c)}$ + H$_{(c)}$] will be discussed elsewhere.[83]

In contrast to dissociative chemisorption at thermal equilibrium, in molecular beam experiments the fractional energy uptakes and $\langle E_j\rangle_R$'s for the different degrees of freedom cannot generally be related to a common effective temperature. Table III provides a listing of f_j, $\langle E_j\rangle_R$, $\langle E_j\rangle$, and $E_a(T_j)$ for our standard molecular beam conditions of Figs. 2, 9, 10,

TABLE III. Dissociative chemisorption for the molecular beam of Fig. 2: Fractional energy uptakes, f_j; mean energy derived from the jth degrees of freedom for complexes undergoing reaction $\langle E_j\rangle_R$; mean energy derived from the jth degrees of freedom for all complexes formed $\langle E_j\rangle$; effective activation energies, $E_a(T_j)=k_b T_j^2 \partial(\ln S)/\partial T_j=\langle E_j\rangle_R-\langle E_j\rangle$.

Mode j	f_j	$\langle E_j\rangle_R$ [eV]	$\langle E_j\rangle$ [eV]	$E_a(T_j)$ [eV]
		$\langle E^*\rangle_R=1.19$ eV	$\langle E^*\rangle=0.87$ eV	
Translation t	0.54	0.64	0.62	
Rotation r	0.008	0.0092	0.0088	0.0004
Vibration ν	0.16	0.19	0.05	0.14
Surface s	0.29	0.35	0.19	0.16

and 11 (NB $E = E^* + E_{ad}$ where $E_{ad} = 0.163$ eV) in which the beam's translational stream energy, $E_b = 0.61$ eV, matches the apparent threshold energy for chemisorption. Once again, the fractional energy uptakes for the molecular beam depend on the relative availability of the different types of energy to contribute to the pooled energy used to surmount the reaction barrier. Here, the beam stream energy is high and the translational energy distribution is constrained by a low temperature, $T_t = 25$ K, forcing $\langle E_t \rangle_R$, $\langle E_t \rangle$, and E_b to be very similar. The much higher temperatures of the molecular vibrational ($T_\nu = 680$ K) and surface oscillators ($T_s = 800$ K) makes these energy reservoirs more flexible. Although molecular translation contributes the most energy towards surmounting the reaction barrier in this example where $E_b = 0.61$ eV and $f_t = 0.54$, if E_b is lowered to 0.2 eV then f_t falls to 0.19 and f_ν and f_s rise to 0.33 and 0.47, respectively. The very low rotational temperatures reached in supersonic molecular beams (ca. 50 K) means that the rotational degrees of freedom are effectively frozen out and contribute little to chemisorption from beams.

VI. CONCLUSIONS

A general framework for analyzing and predicting both thermal equilibrium and nonequilibrium kinetics for surface reactions has been presented and applied to the dissociative chemisorption of methane on Pt(111). The simple physisorbed complex microcanonical unimolecular rate theory (PC–MURT) appears adequate to calculate dissociative sticking coefficients under ordinary equilibrium and nonequilibrium conditions where energy exchange with the surrounding substrate is not overly large. The full Master equation approach (PC–ME) explicitly accounts for vibrational energy exchange with the surface and can generally provide dissociative sticking coefficients and the time and energy dependencies for the physisorbed complex coverage and reactive and desorbing fluxes. For activated dissociative chemisorption, the effect of vibrational energy transfer to the substrate was shown to always shift the sticking coefficient towards its thermal equilibrium value at the surface temperature. In consequence, the apparent threshold energy, E_0, derived from PC–MURT analysis of hyperthermal molecular beam dissociative sticking experiments should constitute an upper bound for the true E_0.

The PC–MURT was used to provide a variety of specific predictions for CH$_4$/Pt(111) dissociative chemisorption and also some more general relationships between experimental measurables [e.g., Eq. (108)] and theory, such as Tolman relations for effective activation energies measured under nonequilibrium conditions. Because surface science and catalysis experiments are often done under nonequilibrium conditions, an important theoretical observation is that experimentally derived quantities such as sticking coefficients, effective activation energies $E_a(T_j)$, or fractional energy uptakes f_j, are often dependent on the very specific experimental details. This may explain, at least in part, some of the apparent differences in experimental findings that have hampered progress towards uniting a theory of gas-surface reactivity with experimental studies of low pressure surface science and high pressure catalysis—a problem sometimes referred to as the "pressure gap."[82]

[1] J.C. Tully, Annu. Rev. Phys. Chem. **51**, 153 (2000).
[2] B. Halpern and M. Kori, Chem. Phys. Lett. **138**, 261 (1987).
[3] A. Danon, A. Vardi, and A. Amirav, Phys. Rev. Lett. **65**, 2038 (1990).
[4] J.B.C. Pettersson, J. Chem. Phys. **100**, 2359 (1993).
[5] V.A. Ukraintsev and I. Harrison, J. Chem. Phys. **101**, 1564 (1994).
[6] C.T. Rettner, H.A. Michelsen, and D.J. Auerbach, J. Chem. Phys. **102**, 4625 (1995).
[7] H. Mortensen, L. Diekhoner, A. Baurichter, and A.C. Luntz, J. Chem. Phys. **116**, 5781 (2002).
[8] P.M. Holmblad, J. Wambach, and I. Chorkendorff, J. Chem. Phys. **102**, 8255 (1995).
[9] L.B.F. Juurlink, P.R. McCabe, R.R. Smith, C.L. DiCologero, and A.L. Utz, Phys. Rev. Lett. **83**, 868 (1999).
[10] H. Yang and J.L. Whitten, J. Chem. Phys. **96**, 5529 (1992).
[11] P. Kratzer, B. Hammer, and J.K. Norskov, J. Chem. Phys. **105**, 5595 (1996).
[12] A.C. Luntz, J. Chem. Phys. **113**, 6901 (2000).
[13] T. Baer and W.L. Hase, *Unimolecular Reaction Dynamics: Theory and Experiments* (Oxford University Press, New York, 1996).
[14] D.G. Truhlar, B.C. Garrett, and S.J. Klippenstein, J. Phys. Chem. **100**, 12771 (1996).
[15] D.C. Chatfield, R.S. Friedman, D.G. Truhlar, B.C. Garrett, and D.W. Schwenke, J. Am. Chem. Soc. **113**, 486 (1991).
[16] W.H. Miller, J. Chem. Phys. **65**, 2216 (1976).
[17] J.H. Larsen and I. Chorkendorff, Surf. Sci. Rep. **35**, 163 (1999).
[18] P.J. Feibelman, B. Hammer, J.K. Norskov, F. Wagner, M. Scheffler, R. Stumpf, R. Watwe, and J. Dumesic, J. Phys. Chem. B **105**, 4018 (2001).
[19] C. Lu, I.C. Lee, R.I. Masel, A. Wieckowski, and C. Rice, J. Phys. Chem. A **106**, 3084 (2002).
[20] B. Gergen, H. Nienhaus, W.H. Weinberg, and E.W. McFarland, Science **294**, 2521 (2001).
[21] W. H. Weinberg, in *Dynamics of Gas-Surface Interactions*, edited by C. T. Rettner and M.N.R. Ashfold (The Royal Society of Chemistry, Cambridge, 1991), Chap. 5.
[22] J. Ding, U. Burghaus, and W.H. Weinberg, Surf. Sci. **446**, 46 (2000), and references therein.
[23] C.T. Reeves, D.C. Seets, and C.B. Mullins, J. Mol. Catal. A: Chem. **167**, 207 (2001), and references therein.
[24] R. Brako and D.M. Newns, Phys. Rev. Lett. **48**, 1859 (1982).
[25] H. D. Meyer and R.D. Levine, Chem. Phys. **85**, 189 (1984).
[26] V. Celli, D. Himes, P. Tran, J.P. Toennies, Ch. Woll, and G. Zhang, Phys. Rev. Lett. **66**, 3160 (1991).
[27] A. Bilic and B. Gumhalter, Phys. Rev. B **52**, 12307 (1995).
[28] J.R. Manson, Phys. Rev. B **58**, 2253 (1998).
[29] F. Hofmann, J.P. Toennies, and J.R. Manson, J. Chem. Phys. **101**, 10155 (1994).
[30] A.C. Luntz and D.S. Bethune, J. Chem. Phys. **90**, 1274 (1989).
[31] M. Head-Gordon, J.C. Tully, C.T. Rettner, C.B. Mullins, and D.J. Auerbach, J. Chem. Phys. **94**, 1516 (1991).
[32] C.B. Mullins, C.T. Rettner, D.J. Auerbach, and W.H. Weinberg, Chem. Phys. Lett. **163**, 111 (1989).
[33] K.A. Holbrook, M.J. Pilling, and S.H. Robinson, *Unimolecular Reactions*, 2nd ed. (Wiley, New York, 1996).
[34] R.G. Gilbert and S.C. Smith, *Theory of Unimolecular and Recombination Reactions* (Blackwell Scientific, Oxford, UK, 1990).
[35] E. Pollak and P. Pechukas, J. Am. Chem. Soc. **100**, 2984 (1978); D.R. Coulson, *ibid.* **100**, 2992 (1978).
[36] J.R. Barker, L.M. Yoder, and K.D. King, J. Phys. Chem. A **105**, 796 (2001).
[37] D.C. Tardy and B.S. Rabinovitch, J. Chem. Phys. **48**, 1282 (1968).

[38] K.F. Lim and R.G. Gilbert, J. Chem. Phys. **84**, 6129 (1986); **92**, 1819 (1990).

[39] A.P. Penner and W. Forst, J. Chem. Phys. **67**, 5296 (1977).

[40] D. Rapp and T. Kassal, Chem. Rev. **69**, 61 (1969).

[41] L.A. Miller and J.R. Barker, J. Chem. Phys. **105**, 1383 (1996).

[42] E. T. Sevy, S.M. Rubin, Z. Lin, and G.W. Flynn, J. Chem. Phys. **113**, 4912 (2000), and references therein.

[43] M.E. Jones, S.E. Roadman, A.M. Lam, G. Eres, and J.R. Engstrom, J. Vac. Sci. Technol. A **13**, 2651 (1995).

[44] M.E. Jones, S.E. Roadman, A.M. Lam, G. Eres, and J.R. Engstrom, J. Chem. Phys. **105**, 7140 (1996).

[45] J.F. Weaver, M.A. Kryzowski, and R.A. Madix, J. Chem. Phys. **112**, 396 (2000).

[46] K. Watanabe, M.C. Lin, Y.A. Gruzdkov, and Y. Matsumoto, J. Chem. Phys. **104**, 5974 (1996).

[47] I. Harrison, Acc. Chem. Res. **31**, 631 (1998).

[48] M.G. Evans and M. Polanyi, Trans. Faraday Soc. **34**, 11 (1938).

[49] V.A. Ukraintsev and I. Harrison, Surf. Sci. **286**, L571 (1993).

[50] C.R. Arumainayagam, M.C. McMaster, G.R. Schoofs, and R.J. Madix, Surf. Sci. **222**, 213 (1989).

[51] J. Harris, J. Simon, A.C. Luntz, C.B. Mullins, and C.T. Rettner, Phys. Rev. Lett. **67**, 652 (1991).

[52] G.R. Schoofs, C.R. Arumainayagam, M.C. McMaster, and R.J. Madix, Surf. Sci. **215**, 1 (1989).

[53] M. Valden, N. Xiang, J. Pere, and M. Pessa, Appl. Surf. Sci. **99**, 83 (1996); M. Valden, J. Pere, M. Hirsimaki, S. Suhonen, and M. Pessa, Surf. Sci. **377–379**, 605 (1997).

[54] T. Beyer and D.R. Swinehart, Commun. ACM **16**, 379 (1973).

[55] G. Herzberg, *Molecular Spectra and Molecular Structure II: Infrared and Raman Spectra of Polyatomic Molecules* (Van Nostrand, New York, 1945).

[56] D.L. Bunker and W.L. Hase, J. Chem. Phys. **59**, 4621 (1973).

[57] K.K. Lehmann, G. Scoles, and B. Pate, Annu. Rev. Phys. Chem. **45**, 241 (1994).

[58] D.J. Nesbitt and R.W. Field, J. Phys. Chem. **100**, 12735 (1996).

[59] A.A. Stuchebrukhov and R.A. Marcus, J. Chem. Phys. **98**, 6044 (1993).

[60] R. Marquardt, M. Quack, and I. Thanopulous, J. Phys. Chem. A **104**, 6129 (2000).

[61] A. Charvat, J. Aßmann, B. Abel, and D. Schwarzer, J. Phys. Chem. A **105**, 5071 (2001).

[62] G. Käb, C. Schröder, and D. Schwarzer, Phys. Chem. Chem. Phys. **4**, 271 (2002).

[63] I. Oref and B.S. Rabinovitch, Acc. Chem. Res. **12**, 166 (1979).

[64] K. Freed, Faraday Discuss. Chem. Soc. **67**, 231 (1979).

[65] R.C. Tolman, J. Am. Chem. Soc. **43**, 2506 (1920).

[66] R. Fowler and E.A. Guggenheim, *Statistical Thermodynamics* (Cambridge University Press, London, 1952).

[67] G.M. McClelland, K.L. Saenger, J.J. Valentini, and D.R. Herschbach, J. Phys. Chem. **83**, 947 (1979).

[68] J.S. Baskin, F. Al-Adel, and A. Hamdan, Chem. Phys. **200**, 181 (1995).

[69] A. Amirav, U. Even, and J. Jortner, Chem. Phys. **51**, 31 (1980).

[70] P.M. Mayer and T. Baer, Int. J. Mass Spectrom. Ion Processes **156**, 133 (1996).

[71] S. Dagan and A. Amirav, J. Am. Soc. Mass Spectrom. **6**, 120 (1995).

[72] M. Schäfer and A. Bauder, Chem. Phys. Lett. **308**, 355 (1999).

[73] C.B. Mullins (private communication).

[74] Y.-K. Sun and W.H. Weinberg, J. Vac. Sci. Technol. A **8**, 2445 (1990).

[75] A.A. Anderson and J.J. Maloney, J. Phys. Chem. **92**, 809 (1988).

[76] C.-T. Au, C.-F. Ng, and M.-S. Liao, J. Catal. **185**, 12 (1999).

[77] E. Shustorovich and H. Sellers, Surf. Sci. Rep. **31**, 1 (1998).

[78] A. Michaelides and P. Hu, J. Am. Chem. Soc. **122**, 9866 (2000).

[79] J.L. Whitten and H.L. Yang, Surf. Sci. Rep. **24**, 55 (1996).

[80] G. Henkelman and H. Jónsson, Phys. Rev. Lett. **86**, 664 (2001).

[81] C.T. Rettner, H.E. Pfnur, and D.J. Auerbach, J. Chem. Phys. **84**, 4163 (1986).

[82] M.B. Lee, Q.Y. Yang, and S.T. Ceyer, J. Chem. Phys. **87**, 2724 (1987).

[83] A. Bukoski and I. Harrison (unpublished).